5-2004

Statistical Mechanical Models of Adsorption and Diffusion of Fluids in Crystalline Nanoporous Materials: Extensions to Percolation and Multicomponent Fluids

Austin M. Newman
University of Tennessee - Knoxville

To the Graduate Council:

I am submitting herewith a thesis written by Austin M. Newman entitled "Statistical Mechanical Models of Adsorption and Diffusion of Fluids in Crystalline Nanoporous Materials: Extensions to Percolation and Multicomponent Fluids." I have examined the final electronic copy of this thesis for form and content and recommend that it be accepted in partial fulfillment of the requirements for the degree of Master of Science, with a major in Chemical Engineering.

David J. Keffer, Major Professor

We have read this thesis and recommend its acceptance:

Brian J. Edwards, Hank D. Cochran

Accepted for the Council:
Dixie L. Thompson

Vice Provost and Dean of the Graduate School

(Original signatures are on file with official student records.)

To the Graduate Council:

I am submitting herewith a thesis written by Austin M. Newman entitled “Statistical Mechanical Models of Adsorption and Diffusion of Fluids in Crystalline Nanoporous Materials: Extensions to Percolation and Multicomponent Fluids”. I have examined the final electronic copy of this thesis for form and content and recommend that it be accepted in partial fulfillment of the requirements for the degree of Master of Science, with a major in Chemical Engineering.

David J. Keffer
Major Professor

We have read this thesis and
recommend its acceptance:

Brian J. Edwards

Hank D. Cochran

Acceptance for the Council:
Anne Mayhew
Vice Chancellor and Dean
of Graduate Studies.

(Original signatures are on file with official student records.)

STATISTICAL MECHANICAL MODELS OF ADSORPTION AND DIFFUSION OF FLUIDS IN CRYSTALLINE NANOPOROUS MATERIALS: EXTENSIONS TO PERCOLATION AND MULTICOMPONENT FLUIDS

A Thesis
Presented for the
Master of Science
Degree
The University of Tennessee, Knoxville

Austin M. Newman
May 2004

DEDICATION

This thesis dedicated to my mother and father, who encouraged me to pursue an advanced degree.

ACKNOWLEDGMENTS

I would like to gratefully acknowledge The Engineering Fundamentals Department for its financial support. Without its help, this thesis would have only been a dream.

I would also like to thank Dr. David Keffer for his cheerful and efficient help in problem solving, computer program debugging, and documenting the work completed in this research project.

ABSTRACT

Kamat et al. has developed an analytical statistical mechanical theory that can be used to model pure component and binary liquid mixtures confined within crystalline nanoporous materials [1, 2]. The theory can be used to predict diffusivities, adsorption isotherms, and heats of adsorption as functions of temperature, pressure, and composition. The predictions obtained from this theory can then be used in macroscopic process level simulations to investigate the use of new adsorbents without conducting expensive experiments.

Kamat et al. has verified that the analytical adsorption theory can be used to model methane confined within zeolite Na-Y [3]. However, the diffusion theory failed to quantitatively model the self-diffusion coefficients for methane confined within Na-Y. Thus, an attempt has been made to improve the fit of the self-diffusion coefficients by incorporating the effects of percolation into the diffusion model. Incorporating the effects of percolation into the diffusion model did not improve the quantitative fit of the self-diffusion coefficients.

The analytical theory is generalizable and can be used for a variety of liquids confined within a variety of nanoporous materials. In this work, the theory is used to model pure component methane and pure component ethane confined within $AlPO_4$-5. The lattice parameters required for the theory are obtained by comparing the theoretical results to results obtained from molecular dynamics simulations. In this work, it has been proven that the theory is generalizable and can be used for different liquids confined within a nanoporous material.

The adsorption theory can also be used to model binary mixtures confined within nanoporous materials. The lattice parameters obtained from the pure component parameter optimizations are used to verify the analytical theory with binary mixtures. Results have been presented which indicate the binary theory does not accurately model a binary mixture confined within nanoporous materials. Problems arise both due to approximations within the theory as well as deviations of the real system from the lattice model.

TABLE OF CONTENTS

LIST OF TABLES

Part 3

Part 4

LIST OF FIGURES

Part 2

Part 3

Part 4

Part 1: Introduction

In the work presented here, the adsorptive and diffusive properties of fluids confined within crystalline nanoporous materials have been investigated. An analytical theory is used to predict the properties of fluids confined in nanopores. The usefulness of the analytical theory is proven with the comparison of the theory results to experimental results obtained from molecular dynamics simulations. The research presented here is divided into three parts. Part 2 is an attempt to improve the accuracy of the self-diffusion coefficients predicted by the original analytical diffusion theory, by incorporating percolation into the lattice model. In Part 3, the usefulness of the analytical theory is verified for two species of liquids confined in a crystalline nanoporous material, $AlPO_4$-5. In Part 4, an attempt has been made to verify the usefulness of the analytical theory for a mixture of two liquids confined within $AlPO_4$-5. Part 5 contains the conclusions of the work presented here.

1.1 Introduction

Nanoporous materials are a class of materials containing pores with a characteristic dimension of a nanometer. Industrial use of nanoporous materials has existed for some time. This class of materials is commonly used as catalysts for chemical reactions. Zeolites, a sub-class of nanoporous materials, have also proven useful for ion exchange. Traditionally, natural nanoporous materials were utilized in industrial processes. However, rapid advances in technology have enabled scientists to synthesize nanoporous materials for industrial uses. In the synthesis of these materials, scientists have been able to create custom-made materials that exhibit specific features such as the size of the pores [4]. The ability to create custom nanoporous materials has provided industry with a plethora of materials to choose from for industrial processes.

With so many materials available for use, it is sometimes extremely difficult to decide which material may provide the best results in an industrial process. Experiments and molecular dynamics simulations can be used to determine how the materials will behave in an industrial process; however, experiments and molecular simulations are very expensive and require a large amount of time to complete. Therefore, there is a need for a single, generic theory, which can be applied to any type of nanoporous material and adsorbent. Kamat et al. have proposed a statistical mechanical theory for the use of nanoporous materials [1-3]. Here an attempt is made to (1) improve the results of the diffusion theory, (2) verify the theory for pure methane and for pure ethane confined within $AlPO_4$-5, and (3) verify the theory for a methane-ethane mixture confined within $AlPO_4$-5.

1.2 Synopsis

In Part 2, the statistical mechanical theory proposed by Kamat et al. is studied. An attempt has been made to improve the results of the diffusion theory by incorporating the effects of percolation into the existing diffusion theory. In this section methane confined within zeolite Na-Y is studied. The original results presented by Kamat et al. are compared to results of the modified percolation-diffusion theory. Incorporating

percolation theory into the diffusion theory was done by using one of the simplest models of percolation, the Effective Medium Approximation (EMA). It has been determined that EMA cannot adequately model the percolative effects of the system. The shortcoming of EMA occurs because this theory assumes the transport blockages are immobile. In this system, the transport blockages are due to adsorbed molecules, which are actually mobile. It is suggested that a percolation model that allows for mobile blockers is required to satisfactorily model diffusion in this system.

In Part 3, the adsorption and diffusion theory is validated for methane and for ethane confined within $AlPO_4$-5. As stated before, using this theory, Kamat successfully modeled adsorption of methane in zeolite-Y, which has a three-dimensional network of roughly spherical cages. To demonstrate the generalizability of this model, it is used to model adsorption of pure methane and pure ethane in $AlPO_4$-5, which has a one-dimensional network of roughly cylindrical channels. Parameters are obtained for the theory by using data points obtained from molecular dynamics (MD) simulations. The results indicate the adsorptive behavior of the fluids can be modeled well, especially at low loadings. However, as was the case with Kamat's work, the prediction of the diffusive behavior is not quantitatively correct.

In Part 4, the theory is applied to a mixture of methane and ethane in $AlPO_4$-5. First, the parameters obtained from the pure component studies in Part 3 are used to model the binary mixture. When these parameters do not yield a satisfactory fit, a new set of parameters is fitted. A satisfactory agreement between the theory and simulation data for either the adsorption or the diffusion phenomena is unattainable. A fundamental flaw in the quasi-chemical approximation has been found which explains why the pure component parameters did not work. It has been suggested that a new set of parameters also failed to model the system satisfactorily most likely due to numerous deviations of the real system from the assumptions of the lattice model.

Part 2: Including Percolation Effects in an Analytical Theory for Diffusion of Fluids in Nanoporous Materials

2.1 Abstract

Kamat et al. have proposed an analytical theory that can be used to model the adsorptive and diffusive behavior of fluids confined within crystalline nanoporous materials [1, 2]. In this work, an attempt is made to improve the fit of the diffusion theory to that of simulation data. Effects due to percolation are incorporated into the diffusion theory via an Effective Medium Approximation (EMA). The goal in this work is to have a simple, easy to use diffusion theory with no parameters. Incorporating EMA into the diffusion theory does not require any parameters. The EMA does not satisfactorily describe the diffusion process. The EMA introduces a diffusion threshold, which occurs at a very low loading. The problem with this work appears to be that the molecules that block motion from one site to the next are themselves mobile. In order to satisfactorily model liquids confined within nanoporous materials, it appears that a more advanced percolation theory that includes blocker mobility is necessary

2.2 Introduction

Kamat et al. have proposed a statistical mechanical theory that can be used to predict the adsorption and diffusion of liquids confined within nanoporous materials [1-3]. The work was completed in three stages: (1) derivation of the adsorption theory, (2) derivation of the diffusion theory, and (3) validation of the adsorption and diffusion theory. In order to validate the theory, methane confined within zeolite Na-Y was modeled. The usefulness and accuracy of the adsorption theory was proven in the methane confined within zeolite Na-Y validation. The diffusion theory predicted the self-diffusion coefficient within the correct order of magnitude of the experimental data and exhibited the same trends apparent in the experimental data. However, there was a desire to improve the quantitative results of the diffusion theory. By incorporating percolation theory into the diffusion theory, it was postulated that the quantitative results of the theory could be improved.

Percolation theory can be used to describe varying numbers of connections in a random network. A square lattice can be used to illustrate the basics of percolation. In Figure (1), a square lattice is presented (All Tables and Figures in Part 2 are in Appendix 1). Some of the lattice sites are connected to each other with a bond. Each bond in the lattice is present with a probability, p. In Figure (1), p is small, thus there are many clusters of small numbers of connected bonds. In this illustration, there is not a network of bonds which spans the entire lattice, thus a fluid would not be able to percolate, or travel through the medium [5]. As the probability of bonds increases, the size of the clusters also increases, whereas the number of clusters decreases. When the probability reaches a certain value, the percolation threshold, p_c, is reached. This is the point at which a fluid can percolate, or travel through the medium [5]. In Figure (1), p is very small and is less than the percolation threshold. In Figure (2), p is greater than the percolation threshold, thus a fluid can percolate or travel through the medium. When p is greater than p_c, there is a connected cluster of sites that spans from one edge of the lattice to the other. This cluster of sites is known as a sample spanning cluster [5]. It is important to note that percolation is very versatile and can be used to model a variety of phenomena. For

example, the same type of lattice model could be used to model the flow of electricity. In the study of nanoporous materials, percolation can be used to model the relationship between the transport properties of a medium and the characteristics of the pathways through which transport occurs.

In this work, a percolation model is incorporated into Kamat et al.'s diffusion model. Much like the original diffusion theory, this extension does not compromise the ease of generalizing the theory for any liquid confined within a nanoporous material. The only requirement for evaluating the theory is the geometry of the nanoporous material, which is already required for the adsorption theory. The intent here is to demonstrate that including percolation into the diffusion theory will improve the fit of the diffusion model.

In Section 2.3, background information about lattice models and percolation is presented. In Section 2.4, the derivation of the percolation extension to Kamat et al.'s theory is presented. Section 2.5 presents the results of the evaluation of the theory with methane confined in zeolite Na-Y. Section 2.6 presents conclusions of the work presented in this chapter.

2.3 Background

2.3.1 Lattice Models

In performing simulations of fluids adsorbed in molecular sieves, it has been determined that localized adsorption sites exist. As a result, lattice models can be used to describe the adsorption of fluids in molecular sieves. These lattice models can incorporate interactions between nearest neighbors. Several researchers have utilized lattice models to describe adsorption of fluids in molecular sieves and zeolites [6-10]. In order to make lattice models more useful, a generalized model has been developed which can be used to describe the adsorption of any fluid in any type of nanoporous material [1-3]. This model can be used to obtain thermodynamic and transport properties of the adsorbed fluid in zeolites. However, the self-diffusion coefficients predicted by the diffusion model were generally 5% - 20% higher than the self-diffusion coefficients obtained from molecular dynamics simulations.

The diffusion model proposed by Kamat in reference [1] obtains local diffusion coefficients at each of the localized adsorption sites. In order to obtain a mean diffusivity, an average of the local diffusion coefficients, weighted by population, is used.

2.3.2 Percolation and the Effective Medium Approximation

Percolation is one of the simplest theories for describing transport in a disordered medium [11]. Several advantages of utilizing a percolation theory include: (1) it is relatively easy to formulate, (2) it can be realistic in qualitative predictions, and (3) it has a minimal dependence on statistics [11]. Percolation theories can be applied to many types of physical phenomena including: supercooled water, galactic structures, fragmentation, porous materials, and earthquakes [5]. In chemical engineering specifically, percolation has been applied to diffusion in zeolites [12]. In the utilization of a percolation model, there are several approaches one may take [13]. In this paper, a bond percolation model is used with an Effective Medium Approximation (EMA). In the past this model has only been used for homogeneous materials [13]. However, the model has

been extended and an attempt has been made to show that it is also applicable for nanoporous materials that contain different types of bond sites.

Percolation has been used successfully to model diffusion in zeolites [12]. Previous work has shown that a percolation model can be used to model diffusion in zeolite A and for the diffusion of benzene in zeolite Y [12]. Therefore, it is reasonable to assume that a percolation model can be integrated with Kamat et al.'s generalized diffusion model to improve the agreement between theory and simulation.

2.4 Theory

A lattice model has been devised which can be used to obtain various thermodynamic properties of an adsorbed fluid in a nanoporous material [1-3]. In this model, the interaction energies are used to obtain local diffusivities, D_i, for each type of move in the lattice. A given type of move depends upon the type of site of origin, the occupancy of the site of origin, the type of the destination site, and the occupancy of the destination site. In the canonical ensemble, the mean diffusivity, D_M, is a function of number of adsorbates, n, number of sites, m, and the temperature, T. The functional form of D_M is

$$D_M(n,m,T) = \sum D_i(x,T)\,p_i(x,n,m)\,. \tag{1}$$

D_i is the local diffusivity of an adsorbate sitting in a site of type i with occupancy x, and temperature, T, and p_i is the weighting function for the corresponding diffusivity, D_i. The diffusivity of each path, or the local diffusivity, is dependent on the activation barrier to motion. The activation energy required for motion is obtained from Kamat's adsorption theory [2]. An example of a specific move would be a molecule present in a site of type 1 with an occupancy of 1, moving to a site of type 2 with an occupancy of 0, and then to a site of type 1 with an occupancy of 0.

In reference [3] Kamat et al. has shown the mean diffusivity obtained in this way does not accurately describe the diffusivity of the adsorbent in the nanoporous material. It is postulated that percolation is occurring and therefore a percolation theory has been incorporated into Kamat et al.'s diffusion theory.

Percolation theories have been used to describe the diffusion of fluids in nanoporous materials [12]. Information available in the literature suggests good agreement of percolation theory to experiments. In the percolation theory, an effective medium approximation can be used to describe the percolation of the adsorbent in the nanoporous material. First, the bond conductance can be described with the following distribution function

$$g(D) = \sum_i p_i \delta(D_M - D_i) \tag{2}$$

where D_M is the mean diffusivity, D_i is the local diffusivity, and p_i is the probability of a move occurring. The summation is required as all types of possible moves are included. Next, the effective medium approximation for the mean diffusivity is

$$\int_0^\infty \frac{D_M - D}{((z/2)-1)D_M + D} g(D)dD = 0, \tag{3}$$

where z is the lattice connectivity, and δ is the Dirac delta function. The lattice connectivity, z, is defined as the number of nearest neighbors of a lattice site. The presence of δ in *g(D)* enables Equation (3) to be evaluated analytically. Upon integration of this function an n^{th} order polynomial is obtained.

The goal in incorporating percolation theory into Kamat et al.'s diffusion theory was to develop a percolation theory that is generalizable and could be applied to any combination of liquid and adsorbent. In the development of this theory, a pattern in the coefficients of the n^{th} order polynomial was identified. The identification of this pattern enabled the development of a computational algorithm that is generalizable and can be used for any combination of liquid and adsorbent. The n^{th} coefficient of the polynomial can be described as

$$c_n = \left(\frac{z}{2} - 1\right)^{n-1} \sum_i p_i \tag{4}$$

where p_i is the probability of a hop occurring. The 0^{th} coefficient can be described as

$$c_0 = \sum_i p_i \left(\prod_j D_j\right) \tag{5}$$

and each of the middle coefficients is

$$c_m = -\left(\frac{z}{2} - 1\right)^m \sum_i p_i D_i f_1 + \left(\frac{z}{2} - 1\right)^{m-1} \sum_i p_i f_{2,i} \ . \tag{6}$$

The function f_1 is

$$\begin{Bmatrix} f_1(m,n) = f_2(m+1,n) \\ f_1(m=n-1,n) = 1 \end{Bmatrix} \begin{matrix} for \quad 0 < m < n-1 \\ for \quad m = n-1 \end{matrix} \tag{7}$$

and f_2 is

$$f_{2,i}(m,n) = \sum_{\substack{j=1 \\ j\neq i}}^{n} D_j \sum_{\substack{k>j \\ k\neq 1}}^{n} D_k \sum_{\substack{i>k \\ l\neq i}}^{n} \ldots \sum_{\substack{m>l \\ m\neq i}}^{n} D_m \ . \qquad (8)$$

The number of summations carried out in $f_{2,i}$ depend on the geometry of the system being studied. The coefficients of the polynomial can be evaluated using a program with recursive subroutines.

This nth order polynomial has, of course, n roots. However, only one of these roots lies in the range of physical values, namely, less than the diffusivity and greater than 0.

2.5 Results and Discussion

In order to utilize the percolation theory, diffusivities and probabilities from the analytical theory presented in reference [1] must be obtained. The system selected for study is methane in zeolite Na-Y.

In Figure (4) Kamat et al. plots simulated and theoretical self-diffusion coefficients (without percolative effects) for methane in zeolite Na-Y as a function of density at five different temperatures [3]. The simulated self-diffusion coefficients and the self-diffusion coefficients proposed by the theory both show an increase in the self-diffusion coefficients with temperature, and a decrease in the self-diffusion coefficients as the density increases. The increase seen with temperature is caused by the self-diffusion's dependence of the activation energy. As the temperature increases, the energetic interactions of the molecules also increase which enables the molecules to more easily overcome the energetic activation barrier. The decrease of the self-diffusion coefficients with increasing density occurs because there are not as many vacant sites for molecules to hop into.

In Figure (5) the theoretical self-diffusion coefficients (with percolation effects) is presented for methane in zeolite Na-Y as a function of density at five different temperatures. The self-diffusion coefficients predicted with percolation exhibit the same temperature dependence as the original diffusion theory. However, the density dependence of the self-diffusion coefficients has changed. As the density increases, the self-diffusion coefficients become 0, in effect, indicating diffusion is not occurring. This phenomenon is observed because there are no longer any sample-spanning clusters. Although this is the behavior expected with percolation, this threshold occurs at a much lower density than expected.

The self-diffusion coefficients predicted with percolation do not qualitatively agree with the MD simulation results. The self-diffusion coefficient curves predicted with percolation have a concave shape which is not present in the MD simulation data.

The percolation model fails to correctly predict the transport functionality on loading. It is believed this occurs because EMA assumes that the blockers are immobile. In this case, since the blockers are adsorbates, they can move; thus a bond is not permanently blocked. A more sophisticated percolation theory that allows for mobile

blockers should model the system better. This more advanced model was not attempted here.

2.6 Conclusions

In this work, an attempt was made to improve upon Kamat et al.'s diffusion theory for fluids confined within nanoporous materials. Methane confined within zeolite Na-Y was the system selected for study.

One of the goals of this project was to incorporate percolation theory into Kamat et al.'s diffusion theory without the use of any additional parameters. This aspect of the research project was successful.

Utilizing percolation in the diffusion model did affect the self-diffusion coefficients as expected. The magnitude of the self-diffusion coefficients at infinite dilution was reduced; however, the self-diffusion coefficients at higher densities reached a threshold of 0 much sooner than expected. The threshold observed is expected when utilizing a percolation model, but in the system presented here the threshold should occur at much higher densities, if at all. Because of this anomaly, it is postulated that a different percolation model should be used for liquids confined within nanoporous materials. Perhaps a theory that allows for mobile blockers may be used to successfully improve the theory's prediction of diffusion of liquids confined within nanoporous materials.

Part 3: Agreement of Adsorption Analytical Theory to Molecular Simulations in $AlPO_4$-5

3.1 Abstract

The statistical mechanical adsorption and diffusion theory, developed by Kamat et. al. [1, 2], is used to model methane and ethane confined within $AlPO_4$-5. As stated before, Kamat successfully used this theory to model adsorption of methane in zeolite-Y, which has a three-dimensional network of roughly spherical cages [3] To demonstrate the generalizability of the model, it is used to model adsorption of pure methane and pure ethane in $AlPO_4$-5, which has a one-dimensional network of roughly cylindrical channels. Parameters are obtained for the theory by fitting to data points obtained from molecular dynamics (MD) simulations. The results indicate the adsorptive behavior of the fluids can be modeled well, especially at low loadings. The theory is seen to capture the fundamental physical mechanisms governing adsorption and fits the simulated data well. The theory captures the temperature and density dependence of the adsorption energies. However, as was the case with Kamat's work, the prediction of the diffusive behavior is not quantitatively correct. The generalizability of parameters such as site volume and site separations in modeling different adsorbates is discussed. This theory provides a practical method to transfer molecular simulation results to macroscopic models.

3.2 Introduction

Over the past twenty years, several research groups have investigated the adsorptive and diffusive behaviors of fluids confined within nanoporous materials. Frequently, molecular simulations are utilized to study these phenomena. Through the use of molecular simulations, much has been discovered about the underlying physical mechanisms of adsorption in nanoporous materials. For instance, it has been demonstrated that competing entropic and energetic effects dictate how adsorbates will be distributed throughout the material. While simulations are an invaluable tool, in order to generate a suite of thermodynamic and transport properties over a range of temperatures, densities, and compositions (required as input in a process-level simulation of, for example, pressure-swing adsorption), many simulations must be run, requiring great computational resources. Because of this limitation of MD simulations, there is a need for a theory which can be fit to a few MD simulations yet still provide accurate interpolation and extrapolation of thermodynamic and transport properties throughout a continuous range of process-operating space, characterized by a range of temperatures, densities, and compositions.

Several analytical, lattice based theoretical models have been developed that describe the adsorption and diffusion in nanoporous materials. For instance, Saravanan et al. have developed an analytical theory for the diffusion of Benzene in Na-Y [14-16]. Van Tassel et al. have developed a lattice theory for the adsorption of small molecules in NaA [8-10]. Another lattice theory has been developed by Snurr et al. for the adsorption of benzene in silicalite [7]. However, these theories are not generalizable and can only be used specifically for the nanoporous material on which they are based.

Recently Kamat et al. have published a series of papers presenting a statistical mechanical theory of adsorption and diffusion in crystalline nanoporous materials [1-3].

This theory is generalizable and can be used for many combinations of adsorbates and nanoporous materials. Another advantage of this theory is the fact that it only requires a minimum number of parameters in order to model a system successfully. In the first three papers of Kamat et al., they derived the adsorptive theory, the diffusive theory, and applied it to methane in zeolite-Y.

In this work, the theory is applied to methane and ethane in the molecular sieve, $AlPO_4$-5. The purpose here is to demonstrate how the theory is generalizable and can be applied to a different adsorbent, with a totally different porous network.

$AlPO_4$-5 , depicted in Figure (1), is a nanoporous aluminophosphate which has a 1-dimensional network of non-intersecting cylindrical pores of approximately 7.3Å [17]. The channels are formed by rings of 12 oxygen, 6 phosphorous, and 6 aluminum atoms. There are 4 adsorption sites in each unit cell of $AlPO_4$-5. Computer simulations have shown that the adsorption lattice is comprised of two types of localized adsorption sites [18]. Simulations have also demonstrated sites of type 1 have a smaller accessible volume, are energetically shallower than sites of type 2, and have a maximum occupancy of one molecule. Sites of type 2 have a larger accessible volume, are energetically deeper, and can be occupied by a maximum of two molecules. These two types of sites alternate down the cylindrical channel, creating a series of deep adsorption sites separated by smaller sites, which present energetic barriers to motion.

In this work, a brief review of the theory is presented in Section 3.3. In Section 3.4, the details regarding the MD simulations are discussed. Section 3.5 presents the results of the evaluation of the theory for methane and ethane adsorbed in $AlPO_4$-5. Section 3.6 presents conclusions obtained from the work.

3.3 Review of Theory

3.3.1 Lattice Model

The statistical mechanical theory of Kamat et al. is based on a lattice model [1, 2]. Using the partition function, thermodynamic and transport properties for the system can be obtained. To completely characterize the lattice, four principle pieces of information must be provided: (1) lattice connectivity, (2) lattice spacing, (3) adsorption site volume, and (4) adsorption site energetic well depth.

In reference [19] it is shown that for a 2-dimensional lattice model, there is no exact analytical solution to the partition function, except for when the fractional loading is 0.5. Therefore, approximations are required in the development of these models. In the development of the model presented here, a conceptually straightforward extension of the traditional quasi-chemical approximation is utilized. The quasi-chemical approximation was selected as it allows for clustering of molecules and resulting phase transitions [19]. The next lower level of simplicity, the Bragg-Williams approximation, does not allow for first-order phase transitions [19]. The traditional quasi-chemical model involved one type of adsorbate, one type of site, and a maximum occupancy of one molecule per site [19]. Kamat et al. extended this model to systems with an arbitrary number of types of sites, where each type of site would vary in terms of site volume, energetic well depth, connectivity to other sites, and maximum occupancy by adsorbate molecules. In order to implement the theory, the lattice connectivity, $\underline{c}$, must be specified . $AlPO_4$-5 can be

modeled with a lattice of two types of sites, $N_T = 2$. One of the types of sites is the main toroidal adsorption site, as shown in the potential energy maps in reference [18]. The second type of site is the energetically unfavorable space between the main sites. Since $AlPO_4$-5 is composed of roughly cylindrical, non-intersecting channels, the connectivity matrix is

$$\underline{c} = \begin{bmatrix} c_{11} & c_{12} \\ c_{21} & c_{22} \end{bmatrix} = \begin{bmatrix} 0 & 2 \\ 2 & 0 \end{bmatrix} \tag{1}$$

where c_{ij} describes the number of sites of type j that are connected to sites of type i. In other words, the channel contains alternating sites of type 1 and type 2.

After constructing the connectivity matrix, three additional parameters must be specified. $\underline{l}$ is the matrix of separation distances between nearest neighbors. $\underline{l}$ has the same form of the connectivity matrix

$$\underline{l} = \begin{bmatrix} l_{11} & l_{12} \\ l_{21} & l_{22} \end{bmatrix} \tag{2}$$

where l_{ij} denotes the separation distance between sites of type j that are connected to sites of type i. The adsorption site energetic well depth, $U_{AP,i}(x)$, is the potential energy due to adsorbate pore interactions and is a function of the occupancy, x, of a site of type, i. For the case where each of the two sites had a maximum occupancy of two adsorbates, the matrix form of U_{AP} is

$$\underline{U_{AP}} = \begin{bmatrix} U_{AP,1}(1) & U_{AP,2}(1) \\ U_{AP,1}(2) & U_{AP,2}(2) \end{bmatrix}. \tag{3}$$

If, as is the case in $AlPO_4$-5, one of the two sites has a maximum occupancy of one, then that element of the matrix need not be defined. The last parameter required in order to describe completely the lattice is $V_{S,i}$, the volume of each type of site, i. In matrix form V_S is represented as

$$\underline{V_S} = \begin{bmatrix} V_{S,1} & V_{S,2} \end{bmatrix}. \tag{4}$$

The partition function consists of three components which include a configurational degeneracy, intrasite partition function, and intersite interaction energy, and has the form of

$$Q(N,M,T) = \sum_{configurations} g(N,\underline{M}) \prod_{i=1}^{N_T} \left[\prod_{x=1}^{m_{s,i}} q_i(x,T)^{x \bullet n_{s,i}(x)} \right] e^{-\sum_{i=1}^{N_T} \sum_{j \geq i}^{N_T} \sum_{x=1}^{m_{s,i}} \sum_{y=1}^{m_{s,j}} N_{ij,xy} \frac{w_x}{kT}}. \tag{5}$$

In the computation of the intersite interaction energy, it is important to note that the only combinations of *i* and *j* of interest are the combinations which have zero neighbors. These combinations are determined by non-zero entries in the connectivity matrix. In completing the summation, care must be taken in not to double count. Another important aspect of the summations is the summation limits noted as $m_{s,i}$ and $m_{s,j}$, which are the maximum occupancies for sites of type *i*, and sites of type *j*. In $AlPO_4$-5, the first site is the small site between the main sites and has a maximum occupancy of 1. The second site is the main site and has a maximum occupancy of 2. Finally, the number of neighbors, $N_{ij,xy}$, defines the number of sites of type *i* with occupancy *x*, that are neighboring sites of type *j* with occupancy *y*. For the specific case of $AlPO_4$-5, there are six different non-zero neighbors of the summation whose indices are presented in Table 1. (All Tables and Figures in Part 3 are in Appendix 2). The intrasite partition function $q_i(x,T)$ has the form

$$q_i(x,T) = \left(\frac{V_{S,i} - xV_A}{x\Lambda^3}\right) e^{-\left(\frac{U_{AP,i} + \frac{x(x-1)}{2} U_{AA,i}}{kT}\right)}, \tag{6}$$

where $V_{s,i}$ is the volume of sites of type *i*, V_A is the volume of the adsorbate, and $U_{AA,i}$ is the adsorbate-adsorbate energy.
The general configurational degeneracy is based on the quasi-chemical approximation and is

$$g(N,M) = \left[\prod_{\substack{i=1 \\ j\neq 1}}^{N_T} \left(\frac{M_i!}{\prod_{x=0}^{m_{s,j}} n_s(x)!}\right)^{(1-c_{ij})}\right]\left[\frac{(c_{12}M_1)!}{\prod_{x=1}^{m_{s,i}}\prod_{y=0}^{m_{s,j}} N_{ij,xy}!}\right]. \tag{7}$$

In order to solve for the partition function, several constraints are used. The constraints used include: (1) site balances, (2) adsorbate balances, (3) symmetry relations for the number of neighbors, and (4) neighbor balances. There are not enough constraint equations to solve for the unknown variables. Therefore, the partition function is minimized with respect to the unknown variables to obtain additional equations. This results in a system of non-linear algebraic equations, which must be solved numerically. The solution of the non-linear equations provides the numerical values of all unknown variables. The partition function can now be evaluated and statistical mechanics can be utilized to obtain the desired thermodynamic properties of the system.

The diffusion process is assumed to be an activated process where a molecule moves from a main site of type 1 (a large site with deep energy well), via a site of type 2 (a small site with shallow energy well) with Arrhenius temperature dependence. Details of the diffusion model are presented by Kamat et al. in reference [1].

3.3.2 External Potential

Up until now, it was assumed that $U_{AP,i}(x)$ is only a function of site occupancy. However, the adsorbate-pore (ap) interaction could in fact be heavily dependent on temperature. The lattice model is flexible enough so any type of external potential can be used. Here a potential is selected that will incorporate temperature dependence into the ap interaction.

The first step is to begin with the local ap interaction energy, $U_{AP,i}(r,x)$, which is a function of occupancy, radius of the pore, and energetic well depth. In evaluating the ap interaction energy, it is important to note, it is assumed that there are spherical sites and spherical adsorbates. The form of $U_{AP,i}(r,x)$ is then given as

$$U_{AP,i}(r,x) = U_{AP,i}(x) + U_{APc,i} \cdot r_i^2 \tag{8}$$

$U_{APc,i}$ is a fitting parameter that had to be incorporate into the potential when the temperature dependence was included. Each type of site will have a $U_{APc,i}$ corresponding to it. The r_i term in the equation is simply the radius of the pore. The volume of each site is known and therefore the radius can be determined by

$$r_i = \sqrt[3]{\frac{3}{4\pi} \cdot V_{s,i}} \ . \tag{9}$$

The Boltzmann Distribution is used to calculate the ap energy for a specific temperature, T as

$$U_{AP,i}(r,x,T) = \frac{\int_{r=0}^{r=r_{\max}} U_{AP,i}(r,x) \cdot r_i^2 \cdot e^{\left(\frac{-U_{AP,i}(r,x)}{k_b T}\right)}}{\int_{r=0}^{r=r_{\max}} r_i^2 \cdot e^{\left(\frac{-U_{AP,i}(r,x)}{k_b T}\right)}} \tag{10}$$

The Boltzmann weighting distribution is included as $e^{\left(\frac{-U_{AP,i}(r,x)}{k_b T}\right)}$. Completing the integration results in

$$U_{AP,i}(r,x,T) = U_{AP,i}(r,x) + \frac{3}{2}k_b T + \frac{U_{APc,i} r_{\max}^2}{1 - \frac{1}{2}\sqrt{\pi}\,\frac{erf\left[r_{\max}\sqrt{\frac{U_{APc,i}}{k_b T}}\right]}{r_{\max}\sqrt{\frac{U_{APc,i}}{k_b T}}\, e^{\left[\frac{r_{\max}^2 U_{APc,i}}{k_b T}\right]}}} \tag{11}$$

This model, Equation (11), has previously been used successfully by Kamat et al. [3]. Including temperature dependence in the adsorbate-pore interaction proved to be necessary in capturing the adsorptive behavior. It introduces one additional parameter, which characterizes the steepness of the energy well.

3.4 Simulations and Numerical Methods

3.4.1 Simulations

The MD simulations performed were completed using the microcanonical ensemble, where number of adsorbates (N), volume (V), and energy (E) remain constant during the simulation [17]. To model the adsorbate-adsorbate (aa) interactions, the Lennard-Jones 20-6 potential model was used:

$$U_{AA} = \sum_{i=1}^{N-1} \sum_{j=i+1}^{N} U_{ij} = \sum_{i=1}^{N-1} \sum_{j=i+1}^{N} 4\varepsilon_{ij} \left[\left(\frac{\sigma_{ij}}{r_{ij}} \right)^{20} - \left(\frac{\sigma_{ij}}{r_{ij}} \right)^{6} \right]. \tag{12}$$

The potential parameters σ and ε are easily obtained from literature and are provided in Table 2.

The simulations included 128 to 256 molecules of the confined fluid. For the lowest simulated density, there are 128 molecules, and 256 unit cells, whereas the highest density simulated requires 256 molecules and 128 unit cells. The long range cut-off distance, r_{cut}, and the neighbor list cut off, $r_{neighbor}$, were 12Å and 18 Å respectively. Other simulation parameters include a 2 fs time step, 10000 equilibration steps, and 100000 data production steps. In order to solve the equations of motion, the 5th-order Gear-Predictor Corrector Method was used [20, 21]. To implement boundary conditions, standard periodic boundary conditions and the minimum image convention were utilized [22, 23].

3.4.2 Numerical Methods

The methodology used in determining the parameters for the lattice model is discussed here. Overall, the values of six parameters which include: $\underline{U_{AP}}$, $\underline{U_{APc}}$, $\underline{V_S}$, and $\underline{l}$ had to be determined. The parameter $\underline{c}$ is not fitted as the information on the geometry of the adsorbate sites can be obtained from a potential energy map.

The objective function is a function that describes the error between the theoretical data and the MD simulation data and is in the form

$$f = \sqrt{\frac{1}{n} \sum_{i=1}^{n} \left(\frac{X_i^{theory} - X_i^{md\_data}}{X_i^{md\_data}} \right)^2}. \tag{13}$$

The X_i denotes the specific data point that is being compared. In the parameter optimizations, it was determined that it is best to first optimize to the ap energy. After the parameters obtained provided a close fit, the aa energy was then used to fine tune the

parameters. When the optimizations were performed with aa energy and ap energy, the weighting factors selected were selected using trial and error. When aa energy was used for fine tuning, its weighting factor was generally 100 times less than the ap energy weighting factor. This is somewhat consistent with the magnitude of the energies, as the aa energy is about 1 order of magnitude less than the ap energy. Other methods of selecting the weighting factors could have been used. However, the method presented here, worked very well. The diffusivity is not used in the parameter optimization process.

The main goal in the optimization process is to minimize the objective function. As the objective function is minimized, the theoretical data approaches the simulation data. Nelder and Mead's Downhill simplex method was used to minimize the objective function [24]. While this method is very robust, it does have one downfall. The success of this method heavily depends on the quality of the initial guess. If the initial guess is not in the correct region, the solution obtained may actually be a local minimum, as opposed to the global minimum. To overcome this downfall, the computational routine is provided with numerous initial guesses. The aim in providing many initial guesses is to insure that the entire domain is searched and the global minimum is found. A single desktop PC can complete the optimization process in only a few minutes.

3.5 Results and Discussion

3.5.1 Parameters

Overall, six scalar parameters had to be determined. The connectivity matrix in Equation (1) is the same for methane and ethane. Clearly the energetic well depth and well steepness parameters are functions of adsorbate identity. Equation (3) shows the matrix form of the energetic well depth. In this matrix, there are what appear to be four unique values of the energetic well depth. However, $U_{AP,1}(2)$ does not exist as sites of type 1 have a maximum occupancy of 1 molecule. In the parameter optimizations, it was determined that the energetic penalty for a doubly occupied site of type 2 was negligible. Therefore,

$$U_{AP,2}(1) = U_{AP,2}(2) \tag{14}$$

which removes the site occupancy dependence from $U_{AP,i}(x)$ and provides the matrix form

$$\underline{U_{AP}} = \begin{bmatrix} U_{AP,1} & U_{AP,2} \\ - & U_{AP,2} \end{bmatrix}. \tag{15}$$

In essence, $U_{AP,i}$ is now only a function of the type of site. In section 3.3.2 it was determined a fitting parameter, $U_{APc,i}$ was necessary when temperature dependence was included in the external potential. Because $U_{AP,i}$ is not a function of the occupancy of a site, $U_{APc,i}$ cannot be a function of the occupancy of a site either. The matrix form of $U_{APc,i}$ is

$$\underline{U_{APc}} = \begin{bmatrix} U_{AP,1} & U_{AP,2} \\ - & U_{AP,2} \end{bmatrix} \tag{16}$$

as $U_{APc,i}$ is only a function of the site type.

Initially it was believed that the site volumes and the site separation matrix could be fixed across adsorbate species. However, the density dependence of the ap interaction required a careful balance of entropic, ap energetic, and aa energetic interactions. The aa interaction is heavily dependent on the separation between sites. In the first attempt at using the theory, potential energy maps were used to obtain the separation distance from the center of one site to the center of another site. However, the sites are large enough that the molecules do not necessarily have to sit in the center of the pore. The repulsive aa interaction due to a molecule in a neighboring site pushes molecules to one side or the other of the site. As a consequence of this aa interaction, it was necessary to fit the site separations and site volumes to each individual species. The site separation distance matrix is presented in Equation (2). $AlPO_4$-5 contains cylindrical channels of alternating adsorption sites. There is no connectivity between a site of type 1 and another site of type 1. Likewise, there is no connectivity between a site of type 2 and another site of type 2. Because of this, l_{11} and l_{22} do not exist for the $AlPO_4$-5 lattice model. The separation distance between a site of type 1, and a site of type 2 is the same as the separation distance between a site of type 2, and a site of type 1. Therefore,

$$\underline{l} = \begin{bmatrix} - & l \\ l & - \end{bmatrix} \tag{17}$$

which reduces the separation matrix to a single parameter, l.

Since the total accessible volume of a unit cell is constant, approximately 360 $Å^3$, and recalling that there are two of each type of site per unit cell, the sum of the site volumes per unit cell were fixed to this total. The model used was based on half of a unit cell which has an accessible volume, V_{acc}, of 180 $Å^3$. Using this constraint, the form of the volume matrix presented in Equation (4) becomes

$$\underline{V_S} = \begin{bmatrix} V_{S,1} & V_{acc} - V_{S,1} \end{bmatrix}. \tag{18}$$

In essence, there is only one independent site volume per species. The parameters obtained for pure component methane and pure component ethane are presented in Tables 5 and 6.

In short, when using this model it is necessary to refit not only the energetic parameters for each species, but also the separation and site volume. An excluded volume factor could perhaps be inserted into the model to remove this necessity. This was not attempted here.

3.5.2 Methane in $AlPO_4$-5

Thirty MD simulations were performed for the adsorption of methane in $AlPO_4$-5 for five densities, ranging from 0.5 to 2 molecules per unit cell, at six different temperatures ranging from 350 to 600 K. The data obtained from the simulations include aa interaction energy, ap interaction energy, total energy, and diffusivity. The MD simulation results are presented in Table 3. In this section, the simulation results are compared to the results obtained from Kamat et al.'s theory.

In Figure (2), a plot of the simulated and theoretical ap interaction energies for methane adsorbed in $AlPO_4$-5 as functions of density at six different temperatures is presented. The simulated energy shows a decrease in the ap energy as a function of density at all temperatures. The physical mechanism responsible for this trend is grounded in the balance between entropic and energetic factors in the free energy. The entropic contribution favors a distribution of molecules in both types of sites. The ap energetic contribution favors all molecules in the energetically deeper sites of type 2. If these were the only two factors influencing the distribution of adsorbates, it would be straightforward to explain the fact that the ap energy increases with temperature, but not the fact that it decreases with loading.

To explain this dependence on loading, one must consider that as the density of the adsorbate increases, the effect of aa interactions becomes increasingly important. The aa interaction is composed of two contributions. The first contribution is due to interactions between a molecule in a site of type 1 and a molecule in an adjacent site of type 2. Based on the value of the separation between these two sites, 3.59 Å (which is less than the methane Lennard-Jones diameter), this intersite aa interaction is repulsive. The second contribution is due to doubly occupied sites of type 2, and is assumed to be at the energy minimum of the Lennard-Jones interaction; thus, this intrasite aa contribution is attractive. However, it is the repulsive intersite aa interaction, that ultimately causes the decrease in ap energy with loading. In Figure (3) data obtained from the theory demonstrates how the ratio of molecules in sites of type 1 (small, shallow) to that of sites in type 2 (large, deep) decreases as loading increases. At very low loadings, there are no substantial aa interactions, so the entropic effect places some adsorbates into unfavorable sites of type 1. However, as loading increases and these sites have neighbors they become even more unfavorable due to the repulsive intersite aa interactions. This additional unfavorableness causes the distribution of adsorbates to shift to the more favorable sites, lowering the ap energy.

One can observe that this model does not perfectly fit the data. There are several reasons for this. First there is noise in the simulation data. This noise occurs because when an MD simulation is conducted, the simulated system must be a finite size, and the simulation must be completed over a finite amount of time. If a MD simulation could be conducted for an infinitely sized system, and for an infinite amount of time, statistical noise would not occur. The simulations conducted were completed for the largest systems possible, and for the longest times possible, based on the computational resources that were available. Second, the lattice model is approximate. Third, the lattice model will become less accurate as loading increases and the premise of the lattice model (i.e. highly localized adsorption sites) becomes less valid.

In Figure (4), the simulated and theoretical aa interaction energies for methane adsorbed in $AlPO_4$-5 as functions of density at six different temperatures is presented. Again, this aa energy includes an attractive intrasite contribution from doubly occupied sites of type 2 and a repulsive intersite contribution from occupied neighboring sites of type 1 and 2. Both the simulated and theoretical energies show a decrease in the ap energy per molecule as a function of density at all temperatures. The disagreement between theory and simulation on a relative scale is large because the aa energy composes only a small portion of the total adsorption energy; the majority of the adsorption energy is due to ap interactions. As a result, the observed disagreement between simulation and theory does not have a significant impact on the total adsorption energy. The agreement between simulation and theory worsens with increasing loading for the same reasons that were given for the ap energy.

In Figure (5), the self-diffusion coefficients as a function of temperature and density are presented. The self-diffusion coefficients predicted by the theory for methane demonstrate the expected dependence on temperature, and the dependence on density. Although the theory agrees in terms of order of magnitude with the simulation data, the quantitative agreement seen here is not good. The diffusion theory utilized here does not require parameters. It would be possible to add parameters to the diffusion theory in order to provide a better fit. However, this would impede the efforts in having a theory with a minimum number of parameters.

In Figure (6) the adsorption isotherms as the average molecules per unit cell versus the chemical potential, μ, of methane at six different temperatures are presented. At low loadings there is very good qualitative and quantitative agreement between the theory and the simulation data. As the loading increases, the data predicted by the theory deviates from the experimental data. This deviation occurs because the premise of the lattice model (i.e. highly localized adsorption sites) becomes less valid.

3.5.3 Ethane in $AlPO_4$-5

As was the case for methane, thirty MD simulations were performed for the adsorption of ethane in $AlPO_4$-5 for five densities, ranging from 0.5 to 2 molecules per unit cell, at six different temperatures ranging from 350 to 600 K. The data obtained from the simulations include aa interaction energy, ap interaction energy, total energy, and diffusivity. The MD simulation results are presented in Table 4. In this section, the MD simulation results are compared to the results obtained from the evaluation of Kamat et al.'s theory.

In Figure (7), the simulated and theoretical ap interaction energies for ethane adsorbed in $AlPO_4$-5 as functions of density at six different temperatures are presented. The simulated energy shows a decrease in the ap energy as a function of density at all temperatures. The same type of physical mechanism responsible for the trends seen with methane confined in $AlPO_4$-5 also governs the behavior of ethane in $AlPO_4$-5. Ethane confined in $AlPO_4$-5 also exhibits the same type of dependence on loading.

In Figure (8), the simulated and theoretical aa interaction energies for ethane adsorbed in $AlPO_4$-5 as functions of density at six different temperatures are presented. Again, this aa energy includes an attractive intrasite contribution from doubly occupied sites of type 2 and a repulsive intersite contribution from occupied neighboring sites of

types 1 and 2. Both the simulated and theoretical energies show a decrease in the ap energy per molecule as a function of density at all temperatures. The agreement between simulation and theory worsens with increasing loading for the same reasons that were presented for the ap energy. Although the theory qualitatively agrees with the simulation data, the quantitative agreement seen here is not very good. One reason for the discrepancy is the fact that when the parameters were fit, the ap interaction energy was more heavily weighted in the objective function. In this case, this is acceptable as the aa interaction energy is only a small contribution to the total energy of the system.

In Figure (9), the self-diffusion coefficients as a function of temperature and density are presented. The self-diffusion coefficients predicted by the theory for ethane demonstrate the expected dependence on temperature, and the dependence on density. Although the theory agrees in terms of order of magnitude estimates with the simulation data, the quantitative agreement seen here is not good. The diffusion theory utilized here does not require parameters. It would be possible to add parameters to the diffusion theory in order to provide a better fit. However, this would impede the efforts in having a theory with a minimum number of parameters.

In Figure (10) the adsorption isotherms as the average molecules per unit cell versus the chemical potential of ethane at six different temperatures are presented. The adsorption isotherms predicted by the theory exhibit poor qualitative and quantitative agreement with the molecular dynamics simulation data. It is speculated this disagreement occurs because the premise of a lattice model becomes less valid when modeling larger adsorbates.

3.6 Conclusions

In this work, Kamat et al.'s adsorption theory was used to model adsorption and diffusion of pure methane in $AlPO_4$-5 and pure ethane in $AlPO_4$-5. The lattice parameters required for the theory are obtained by fitting the ap energy from the theoretical results to results obtained from molecular dynamics simulations.

The theory is very computationally efficient, generating data that would require thousands of hours of computer time for MD simulations. The theory is very simple to implement, requiring only six fitting parameters for the adsorption data, and no parameters for the self-diffusion coefficients.

The theory accurately predicted results for the aa energy for methane confined in $AlPO_4$-5, and for ethane confined in $AlPO_4$-5. However, there were several anomalies discovered in the theory, mainly the inability to predict accurately the aa-interactions at high loadings, which is a small contribution to the total adsorption energy. Also demonstrated is the poor quantitative agreement of the predicted self-diffusion coefficients. The adsorption isotherms for methane were modeled quite well at low densities whereas the theory failed to correctly model the adsorption isotherms for ethane at any loading. However, it is believed that the theory will provide a practical platform by which a continuous range of thermodynamic properties (not necessarily the transport properties) can be obtained from a few simulation results, so that this information can be utilized in a process-level simulation.

Part 4: A Statistical Mechanical Model of Binary Mixtures Confined in Nanoporous Materials

4.1 Abstract

Kamat et. al's statistical mechanical theory of adsorption and diffusion in nanoporous materials is applied to a mixture of methane and ethane in $AlPO_4$-5. First, the parameters obtained from the pure component studies in Part 3 are used to model the binary mixture. When these parameters do not yield a satisfactory fit, a new set of parameters is fitted. A satisfactory agreement between the theory and simulation data for either the adsorption or diffusion phenomena is unattainable. A fundamental flaw in the quasi-chemical approximation has been found that explains why the pure component parameters did not work. It has been suggested that a new set of parameters also failed to model the system satisfactorily most likely due to numerous deviations of the real system from the assumptions of the lattice model.

4.2 Introduction

Recently Kamat et al. have demonstrated the use of a statistical mechanical theory that can be used to predict the adsorption and diffusion of liquids in crystalline nanoporous materials. In the papers, Kamat et al. present the derivation of the adsorptive theory, the diffusive theory, and then validate the theory using methane in zeolite-Y [1-3]. In Part 3 of this paper, the theory has been applied to methane in $AlPO_4$-5 and to ethane in $AlPO_4$-5. Part 3 of this paper has proven how the theory is generalizable and can be used for different liquids and materials. However, in many cases, engineers may be interested in binary mixtures confined within nanoporous materials.

In this work, an extension to the theory is used. The extension to the theory enables the modeling of a binary mixture confined within a nanoporous material. Much like the single component theory, the extension does not compromise the ease of generalizing the theory for any type of liquid confined in any type of nanoporous material. Here the aim is to model a methane/ethane mixture confined within $AlPO_4$-5. The purpose here is to demonstrate how the parameters obtained from the single-component parameter optimizations can be used to evaluate the binary mixture theory.

A brief review of the theory is presented in Section 4.3 of this paper. In Section 4.4, the details regarding the MD simulations are discussed. Section 4.5 presents the results of the evaluation of the theory for methane and ethane adsorbed in $AlPO_4$-5. Section 4.6 presents conclusions obtained from this work.

4.3 Review of Theory

4.3.1 Lattice Model

The statistical mechanical theory proposed by Kamat et al. is based on a lattice model. To completely characterize the lattice, four parameters are required: (1) lattice connectivity, (2) lattice spacing, (3) adsorption site volume, and (4) adsorption site energetic well depth. After the parameters are specified, the model can be used to obtain a partition function. The partition function can then be used to obtain any thermodynamic properties of the system.

The partition function consists of three components including a configurational degeneracy, intrasite partition function, and intersite interaction energy,

$$Q(N_1, N_{2,}M,T) = \sum_{configurations} g(N_1, N_2, \underline{M}) * qterm * eterm \quad (1)$$

where *g* is the configurational degeneracy, *qterm* is the intrasite partition function, and *eterm* is the intersite interaction energy.
The general configurational degeneracy is based on the quasi-chemical approximation:

$$g(N_1, N_2, M) = \left[\prod_{\substack{i=1 \\ j\neq 1}}^{N_T} \left(\frac{M_i!}{\prod_{x=0}^{m_{s,j}} \prod_{y=0}^{m_{s,j}} n_{s,i}(x,y)!} \right)^{(1-c_{ij})} \right] \left[\frac{(c_{12}M_1)!}{\prod_{x=0}^{m_{s,i}} \prod_{y=0}^{m_{s,j}^*} \prod_{w=0}^{m_{s,i}} \prod_{z=0}^{m_{s,j}^*} N_{i,j}(x,y,w,z)} \right] \quad (2)$$

where $n_{s,i}(x,y)$ is the number of sites of type *i* with occupancy *x* of component 1 and occupancy *y*, of component 2. The neighbor variables use the same notation where $N_{i,j}(x,y,w,z)$ is the number of sites of type *i* with occupancy *x* of component 1 and occupancy *y*, of component 2 that neighbor sites of type *j* with occupancy *w* of component 1 and occupancy *z*, of component 2. The asterisk in the equation indicates the total occupancy of the site does not exceed the accessible volume.
The intrasite partition function for a binary mixture slightly differs slightly from the single component function and has the form of

$$qterm = \prod_{i}^{N_T} \prod_{x=0}^{m_{s,i,1\max}} \prod_{y=0}^{m_{s,i,2\max}^*} [q_{i,1}(x,y,T)^x q_{i,2}(x,y,T)^y]^{n_{s,i(x,y)}} . \quad (3)$$

Here it is important to note that $q_{i,f}(x,y,T)$ is the intrasite partition function for a site of type *i* for component *j*, with an occupancy *x* for the first adsorbed species and occupancy *y* for the second adsorbed species. It is also important to understand the limits on the product, $m_{s,i,1max}$ and $m_{s,i,2max}$. $m_{s,i,1max}$ is the maximum occupancy of component 1 in a site of type *i* and $m_{s,i,2max}$ is the maximum occupancy of component 2 in a site of type *i*. The first component of the intrasite partition has the form

$$q_{i,1}(x,y,T) = \left(\frac{V_{s,i} - (xV_a(1) + yV_a(2))}{(x\Lambda_1^3 + y\Lambda_2^3)} \right) e^{-\left(\frac{\frac{x(x-1)}{2} w_i(1,1) + \frac{xy}{2} w_i(1,2)}{kT} \right)} . \quad (4)$$

$V_{s,i}$ is the volume of a site of type *i*, *x* is the number of adsorbates of component 1, *y* is the number of adsorbates of component 2, V_a is the volume of the adsorbate, Λ is the thermal deBroglie wavelength, $w_i(k,m)$ is the interaction energy between a molecule of component *k* and a molecule of component *m* sitting in a neighboring site, *T* is the

temperature in Kelvin, and *k* is the Boltzmann constant. The second component of the intrasite partition function is

$$q_{i,2}(x,y,T) = \left(\frac{V_{s,i} - (xV_a(1) + yV_a(2))}{(x\Lambda_1^3 + y\Lambda_2^3)} \right) e^{-\left(\frac{\frac{y(y-1)}{2} w_i(2,2) + \frac{xy}{2} w_i(1,2)}{kT} \right)}. \quad (5)$$

Constraints for the intrasite partition function must be used in order to prevent: (1) double counting, and (2) the use of a configuration where the volume of the adsorbates is larger than the site volume. The intersite (nearest neighbor) energetic term of the partition function is given by

$$eterm = e^{\sum_{i=1}^{N_T} \sum_{j\geq 1}^{N_T} \sum_{x=0}^{m_{s,i}} \sum_{y=0}^{m_{s,i}^*} \sum_{w=0}^{m_{s,j}} \sum_{z=0}^{m_{s,j}^*} N_{i,j}(x,y,w,z) \left(\frac{(xw)w_{11} + (xz+yw)w_{12} + (yz)w_{22}}{kT} \right)}, \quad (6)$$

where the variable naming conventions presented above are used.

Compared to the pure component lattice model, the binary mixture has more types of adsorbed sites, and more types of possible neighbors. For example, there may be a site of type *i* with occupancy *x* of component 1 and occupancy *y* of component 2 neighboring a site of type *j* with occupancy *w* of component 1 and occupancy *z* of component 2. Compared to the single component model, the partition function for a binary mixture confined in $AlPO_4$-5 increases the types of sites from 5 to 9, and the types of site neighbors from 6 to 18. Each of these variables must be determined from a set of nonlinear algebraic equations.

The solution process for the binary mixture partition function is the same as for the single component partition function. As Kamat et al. have presented, constraints for the system must be provided. More constraints must be defined because of the additional neighbor variables, and types of adsorbed sites. As before, the constraints take four forms: (1) site balances for each type of site, (2) adsorbate balances for each component, (3) neighbor balances for each combination of site and occupancy, and symmetry relations. These constraints do not provide enough information to determine uniquely all of the unknown variables. The partition function is then minimized with respect to the remaining independent variables. This results in a system of non-linear algebraic equations which must be solved numerically. The solution of these equations provides numerical values of the unknown variables which can then be used to evaluate the partition function.

The diffusion theory did not need to be extended as it is based on the activated energy of motion which the adsorption theory provides for each component in the binary mixture. Details of the diffusion model are provided by Kamat et al. in reference [1].

4.3.2 External Potential

Any type of external potential can be used in the lattice model. Kamat et al. have discussed the necessity of including temperature dependence in the adsorbate-pore

energetic interactions. The model used for the external potential is presented in Section 3.3.2.

4.4 Simulations and Numerical Methods

4.4.1 Simulations

The MD simulations performed were completed using the micro-canonical ensemble, where number of adsorbates (N), volume (V), and energy (E) remain constant during the simulation. The simulation data is presented in Table 1. [17, 25] (All Tables and Figures in Part 3 are in Appendix 3).

4.4.2 Numerical Methods

The expectation was that using the parameters fitted to pure component simulation data for adsorption site volume, $V_{s,1}$, adsorption site energetic well depth, U_{AP}, and adsorption site energetic well steepness, U_{APc}, and using simple mixing rules for interaction energies between components, the mixture should be modeled reasonably well. The interaction energies are obtained through the use of the Lennard-Jones equation of state. Therefore, mixing rules are used for the Lennard-Jones parameters σ and ε where

$$\sigma_{MIX} = \frac{(\sigma_1 + \sigma_2)}{2} \tag{7}$$

and

$$\varepsilon_{MIX} = -\sqrt{(\varepsilon_1 + \varepsilon_2)}\,. \tag{8}$$

In the single component case, it was assumed that there was no energetic penalty for double occupancy of a site. This assumption was made solely to limit the number of independent parameters in the model. In the binary mixture, this assumption is used and extended to doubly occupied sites with one methane and one ethane. For methane and ethane, the energetic well depth, U_{AP}, used for the binary mixture was

$$U_{AP,Me,2}(x=1,y=0) = U_{AP,Me,2}(x=2,y=0) = U_{AP,Me,2}(x=1,y=1) \tag{9}$$

and

$$U_{AP,Et,2}(x=1,y=0) = U_{AP,Et,2}(x=2,y=0) = U_{AP,Et,2}(x=1,y=1) \tag{10}$$

where $U_{AP,Me,i}(x{=}1,y{=}1)$ and $U_{AP,Et,i}(x{=}1,y{=}1)$ are the energetic well depths obtained from the pure component parameter optimization. x is the occupancy of methane in the site, and y is the occupancy of ethane in the site. In essence, the same well depth is used for singly and doubly occupied sites. The energetic well steepness, U_{APc}, is treated in a similar fashion where

$$U_{APc,Me,2}(x=1,y=0)=U_{APc,Me,2}(x=2,y=0)=U_{APc,Me,2}(x=1,y=1) \quad (11)$$

and

$$U_{APc,Et,2}(x=1,y=0)=U_{APc,Et,2}(x=2,y=0)=U_{APc,Et,2}(x=1,y=1) \quad (12)$$

as the well steepness is only a function of the site type.

In the pure component case, it was necessary for each pure component to have a unique separation distance for intersite interactions. For the binary mixture, the separation distance for Me-Me and Et-Et interactions are the same as they were in the pure component cases. The separation distance for Me-Et interactions, l_{mix}, was obtained by using the following mixing rule

$$l_{mix}=\frac{l_{Me}+l_{Et}}{2} \quad (13)$$

As a reminder, different site volumes were fit for the two pure component cases. In the mixture, only one value of the volume of each type of site can be used. In order to determine the site volume to be used in the mixture, the average of the pure component results were initially used. However, the results achieved using this methodology did not accurately portray the behavior of the system.

The second attempt at estimating the site volumes to be used in the mixture without refitting them, was to simultaneously optimize the volumes to both pure component methane and pure component ethane data. This required a re-optimization of all of the independent parameters. The parameters obtained in this re-optimization qualitatively and quantitatively described the behavior of the pure component system. However, the fits obtained for the pure component data using this methodology were not as good as the results presented in Part 3 of this paper. The parameters obtained from the simultaneous optimization are the parameters initially used for the binary mixture and are presented in Tables 2. and 3.

A third procedure was also used to generate parameters for the binary system, which was to completely fit a new set of parameters to the binary case. This is, of course, not the desired procedure. It would be much more desirable to be able to estimate the mixture parameters from the pure component parameters. However, it is instructive to see how well the model can predict binary behavior, given optimal parameters. The optimization process for a binary mixture is completed using the same methodology as described by Kamat, et al. for the single component model [3]. The methodology for the parameter optimization is presented in Section 3.4.2. As in the pure component case, a single desktop PC can complete the optimization process in only a few minutes. The parameters obtained in this procedure are presented in Tables 4. and 5.

4.5 Results and Discussion

4.5.1 Parameters

Overall, eleven parameters had to be used to characterize completely a binary mixture. The connectivity matrix used for the binary mixture is

$$\underline{c} = \begin{bmatrix} c_{11} & c_{12} \\ c_{21} & c_{22} \end{bmatrix} = \begin{bmatrix} 0 & 2 \\ 2 & 0 \end{bmatrix} \tag{14}$$

which is the same matrix used for the pure component lattice model. The site volume matrix used for the binary mixture is

$$\underline{V_S} = \begin{bmatrix} V_{S,1} & V_{acc} - V_{S,1} \end{bmatrix} \tag{15}$$

where V_{acc} is 180 Å^3. This is the same format used for the pure component case. It is important to recall the pure component optimizations resulted in a different site volume for the pure component methane and for the pure component ethane. In Section 4.4.2, there was a discussion of the pure component simultaneous re-optimization that yielded one unique volume. It is also important to recall that the volume of sites of type 2 is constrained by the volume available in the unit cell and therefore is a function of the volume of sites of type 1.

In the parameter re-optimization the separation distance, *l*, remained unique for each adsorbed species. Therefore, there will be two *l,* matrices, one for methane, and one for ethane. These matrices have the same form as in the pure component case which is

$$\underline{l} = \begin{bmatrix} - & l \\ l & - \end{bmatrix}. \tag{16}$$

The treatment of the energetic well depth, U_{AP}, and the energetic well steepness, U_{APc} for the binary mixture model was discussed in Section 4.4.2. The U_{AP} matrix for a binary mixture is

$$\underline{U_{AP}} = \begin{bmatrix} U_{AP,1} & U_{AP,2} \\ - & U_{AP,2} \end{bmatrix} \tag{17}$$

where $U_{AP,1}$ is the energetic well depth for a molecule in a site of type 1, and $U_{AP,2}$ is the energetic well depth for a molecule in a site of type 2. There will be two U_{AP} matrices for the binary mixture model, one for methane, and one for ethane. The U_{APc} matrix for a binary mixture is

$$\underline{U_{APc}} = \begin{bmatrix} U_{APc,1} & U_{APc,2} \\ - & U_{APc,2} \end{bmatrix} \tag{18}$$

where U_{AP} is the energetic well steepness for a molecule in a site of type 1, and $U_{APc,2}$ is the energetic well steepness for a molecule in a site of type 2. There will be two U_{APc} matrices for the binary mixture model, one for methane, and one for ethane.

In the initial evaluation of the binary model, the eleven parameters were obtained from the pure component parameter optimizations. However, the pure component parameters failed to model accurately the behavior of adsorption in a binary mixture. Therefore, the parameters were re-optimized using the binary lattice model.

4.5.2 50% Methane/50% Ethane Mixture in $AlPO_4$-5

Thirty MD simulations were performed for the adsorption of the 50% methane/ 50% ethane mixture in $AlPO_4$-5 for five densities, ranging from 0.5 to 2 molecules per unit cell, at six different temperatures ranging from 350 to 600 K. The simulations have provided adsorbate-adsorbate (aa) interaction energy, adsorbate-pore (ap) interaction energy, total energy, and diffusivity. In this section, the simulation results are compared to the results obtained from the evaluation of the theory.

In Figure (2), the simulated and theoretical ap interaction energies for the binary mixture adsorbed in $AlPO_4$-5 as functions of density at six different temperatures are presented. The lattice parameters obtained from the pure component model simultaneous optimization were used here and are presented in Tables 2. and 3. The simulated ap energetic interactions show a decrease in the ap energy as a function of density at all temperatures and an increase in ap energy with an increase in temperature. The physical mechanism responsible for the increase in ap energy as the temperature increases is based upon the balance of entropic contributions and ap energetic contributions to the free energy. The entropic contributions tend to place the adsorbed molecules equally in both types of sites. The ap energetic contributions tend to place the adsorbed molecules in the energetically deeper sites of type 2. These contributions only explain the temperature dependence of the ap interaction energy.

The dependence on density occurs because as the density increases, the aa interactions become increasingly important. The aa interactions consist of two components; intrasite interactions that occur between an adsorbed molecule in a site of type 1 with a molecule in a site of type 2, and intersite interactions that occur between two molecules in a site of type 2. The intrasite interactions are repulsive as the separation distance between the two separate sites is approximately 3.84 Å (which is less than the methane or ethane Lennard-Jones diameter). The intersite interactions are assumed to be at the energetic minimum of the Lennard-Jones interaction, thus this aa interaction is attractive. However, the repulsive aa intrasite interactions dominate which ultimately causes the decrease in ap energy with loading.

In Figure (2) the theory does not provide a good fit to the simulation results. The theory predicts the ap energy increases as a function of density. It is apparent that the theory is not capturing the actual physical mechanism responsible for adsorption. This failure is also apparent in the aa interaction energy which is plotted in Figure (3). In Figure (3), the simulated aa interaction energy for the binary mixture adsorbed in $AlPO_4$-5 as a function of density at six different temperatures is presented. Here the theory presents strongly repulsive energetic interactions. Figure (3) reaffirms the fact the theory

is not capturing the actual physical mechanism responsible for adsorption when the pure component parameters are used.

The source of this breakdown lies in the quasi-chemical approximation. The shortcoming in the quasi-chemical approximation is most easily illustrated by considering a simple case with one type of site, one adsorbate component, and a maximum occupancy of one. In this case, the configurational degeneracy that would appear in the partition function, Equation (1), is given by

$$g = \left(\frac{M!}{n_s(0)!n_s(1)!} \right)^{(1-c_{11})} \left(\frac{\left(\frac{c_{11}}{2} M \right)!}{N_{00}!N_{11}!\left(\frac{N_{01}!}{2} \right)^2} \right) \tag{19}$$

where $n_s(0)$ denotes sites with 0 occupancy, and $n_s(1)$ denotes sites with an occupancy of 1[19]. The neighbor variables follow the same convention where N_{00} is the number of sites with occupancy 0 neighboring a site with occupancy 0, N_{11} is the number of sites with occupancy 1 neighboring a site with occupancy 1, and N_{01} is the number of sites with occupancy 0 neighboring sites with occupancy 1.

Now consider the same case except that there are two components, which are identical. The fact that there are two distinguishable components should have an effect on the entropy of the system but not on the energy. The configurational degeneracy for this case is given by

$$g = \left(\frac{M!}{n_s(0)!n_s(A)n_s(B)} \right)^{(1-c_{11})} \left(\frac{\left(\frac{c_{11}}{2} M \right)!}{N_{00}!N_{AA}!N_{BB}!\left(\left(\frac{N_{AB}!}{2} \right)\left(\frac{N_{0A}!}{2} \right)\left(\frac{N_{0B}!}{2} \right) \right)^2} \right). \tag{20}$$

Now, if the assumption is made that component A is the same as component B, Equation (19) will become

$$g = \left(\frac{M!}{n_s(0)!\left(n_s(A)+n_s(B)\right)} \right)^{(1-c_{11})} \left(\frac{\left(\frac{c_{11}}{2} M \right)!}{N_{00}!\left(N_{AA}+N_{BB}+\frac{N_{AB}}{2} \right)!\left(\frac{N_{0A}+N_{0B}}{2} \right)!^2} \right). \tag{21}$$

Equation (21) and Equation (19) are not the same, nor should they be. The entropy of a mixture is different from the entropy of the pure system. The problem is that in the quasi-chemical approximation used for this model, all properties (both entropic and energetic) are determined by minimizing the partition function with respect to independent site variables, n_s, and independent, neighbor variables. The values of these variables are, in the general case, different. Thus, all thermodynamic properties generated by the partition

function are different. In other words, the quasi-chemical approximation used in this model has an inherent flaw which does not allow it to be used for both pure component and mixture systems. The energy of a mixture of species that are identical in all characteristics but labeling is not the same as the energy of a pure component of a species with those same properties. This flaw in the quasi-chemical approximation does not become apparent until N_T=2, and there are now two different types of sites (with different energy levels) in which the adsorbates can be distributed. Because of this disagreement, the parameters obtained by fitting to the pure component simulation data could not be used in the evaluation of the theory for a binary mixture.

Even though this disagreement exists, an attempt was made to re-optimize the parameters for the binary mixture. First, an attempt was made to re-optimize only to the site volume and the site separation distance. However, this methodology did not provide a good fit. It became necessary to re-optimize all the parameters. The re-optimized parameters are presented in Tables 4. and 5.

In Figure (4), the simulated ap interaction energy for the binary mixture adsorbed in $AlPO_4$-5 as a function of density at six different temperatures is presented. Here it is apparent that the binary optimized parameters' agreement between the simulation data and the results presented by the theory has improved. However, the theoretical data demonstrate an increase in ap interaction energy as the density increases. The trend occurs because of the way the sites have been filled. At lower densities, one would expect the entropic energetic effects to place molecules in the unfavorable sites of type 1. However, in the binary model, the energetic effects are greater than the entropic effects and the sites of type 1 remain empty. In reviewing the results presented by the model it is believed, the actual physical mechanisms responsible for the adsorption of a binary mixture in $AlPO_4$-5 have not been captured.

In Figure (5), the simulated aa interaction energies for the binary mixture adsorbed in $AlPO_4$-5 as a function of density at six different temperatures with the new parameter set are presented. The site volumes and the site separation distance were optimized and are the same parameters used in Figure (4). Here the aa interaction energy is slightly attractive and has a good quantitative agreement with the simulated aa interaction energy. However, the aa interaction is only a small component of the total energy present in the system. Therefore, the disagreement within the ap interaction energy dominates the total behavior of the system.

In Figure (6), the ratio of occupied sites of type 1 to the ratio of occupied sites of type 2 at six different temperatures is presented. Here the number of sites of type 2 increase with loading. As previously discussed, the number of sites of type 1 at lower densities should be greater. However, the energetic effects of the model overshadow the entropic effects so a greater number of sites of type 1 at lower densities is not observed.

It is believed that there are two inadequacies in the theory that prevent it from predicting the correct behavior. One of the causes is one that has already been discussed, the failure of the binary partition function reducing to the single-component partition function. The other cause are nuances of the lattice model. In the simulations, the adsorbed molecule has an accessible volume in which it can sit in a site. The accessible volume is dependent on the size of the site and the adsorbate. The lattice model is much more stringent in this matter, especially when larger adsorbates are involved.

It is believed the deviations from the lattice model were probably always present, even in the single-component case. However, the deviations were accounted for by varying volume and separation distance. However, in the binary case, the deviations take forms that are more complex and these deviations cannot be accounted for with the given parameters in this model.

In Figure (7), the self-diffusion coefficients for methane in the binary mixture as a function of temperature and density are presented. The self-diffusion coefficients predicted by the theory for methane do not qualitatively or quantitatively model the MD simulation data. Most likely, this occurs because the lattice diffusion model is dependant on the interaction energies obtained from the lattice adsorption model. The performance of the lattice adsorption model for a binary mixture has already been discussed. The ethane self-diffusion coefficient exhibited the same behavior as the methane self-diffusion coefficient.

4.6 Conclusions

In this work, an attempt was made to apply Kamat et. al's adsorption and diffusion theories for a binary mixture of methane and ethane in $AlPO_4$-5. Good qualitative agreement between simulation data and the prediction of the theory was not obtained. It is apparent that the lattice theory incorporating the quasi-chemical approximation, while satisfactory for pure components, does not describe the adsorption and diffusion behavior of binary mixtures in $AlPO_4$-5 well.

The reasons the theory did not accurately predict the behavior of a binary mixture confined within a nanoporous material have been discussed. In order to successfully model a binary mixture using parameters obtained from a pure component model, a lattice theory that predicts the same energy for the pure component and for a mixture of two identical components would have to be used. The prediction of the theory was improved after the parameters were re-optimized for the binary model. However, it is believed nuances, which are also present in the pure component case (but could be accounted for in the pure component case), became more pronounced and prevented the binary model from accurately modeling the binary system.

Part 5: Conclusion

In this work, an analytical theory for adsorption and diffusion in nanoporous materials has been modified and applied to several combinations of adsorbates and adsorbents. In this section, a summary of what has been discovered is presented. A discussion of what can be completed in order to improve upon the results is also presented.

5 Conclusion

In Part 2, the statistical mechanical theory proposed by Kamat et al. is studied. An attempt has been made to improve the results of the diffusion theory by incorporating the effects of percolation into the existing diffusion theory. In this section, results obtained by Kamat et al. were compared to results obtained with percolation incorporated into Kamat et al.'s lattice diffusion theory. Percolation theory was selected for this study as it has previously been used successfully to model diffusion in zeolites. Incorporating percolation theory into the diffusion theory was done by using one of the simplest models of percolation, Effective Medium Approximation (EMA). The percolation model reduced the magnitude of the self-diffusion coefficients as expected. However, the percolation threshold point was reached at a much lower density than expected. This is the point at which percolation along the lattice cannot occur, thus the self-diffusion coefficients become 0. It has been determined that EMA cannot adequately model the percolative effects of the system. The shortcoming of EMA occurs because this theory assumes the transport blockages are immobile. In this system, the transport blockages are due to adsorbed molecules, which are actually mobile. In order to successfully incorporate percolation into Kamat et al.'s lattice diffusion model, a more advanced percolation theory would have to be used. It is suggested that a percolation theory that allows for mobile blockers should be used for future work.

In Part 3, the adsorption and diffusion theory is validated for methane and for ethane confined within $AlPO_4$-5. Kamat et. al. has successfully modeled adsorption of methane in zeolite-Y, which has a three-dimensional network of roughly spherical cages. To demonstrate the generalizability of this model, it is used to model adsorption of pure methane and pure ethane in $AlPO_4$-5, which has a one-dimensional network of roughly cylindrical channels. Parameters are obtained for the theory by fitting to the results of molecular dynamics (MD) simulations. The theory was used to generate adsorbate-pore (ap) energies, adsorbate-adsorbate (aa) energies, self-diffusion coefficients, and adsorption isotherms. The ap energies, and the aa energies were modeled well, especially at low loadings. However, as was the case with Kamat et al.'s work, the prediction of the self-diffusion coefficients is not quantitatively correct. The methane adsorption isotherms were modeled well at low loadings. The ethane isotherms did not agree with the data from the MD simulations nearly as well as methane. It is believed this adsorbate dependence in the model is a result of the fact that the ethane is a larger molecule and thus the correction due to excluded volume (which was not included in this work) would have more of an impact. However, because of the good agreement seen with the ap and aa energies, it is believed the theory can provide a practical platform by which a continuous range of thermodynamic properties can be obtained for the use in process level simulations.

In Part 4, a binary mixture of methane and ethane confined within $AlPO_4$-5 is studied. Kamat et al. have provided an expansion of their statistical mechanical lattice theory which can be used for binary mixtures. The lattice parameters obtained in the parameter optimizations from Part 3 were used in the binary model. The parameters used did not provide a qualitative or quantitative agreement between the theory and simulation data. Therefore, it was deemed necessary to fit a new set of parameters using the binary mixture model. The new parameters helped to improve the fit of the theory. However, even with the new set of parameters the theory did not qualitatively model the data obtained from the MD simulations. After careful study, it was determined the quasi-chemical approximation prevented the use of the pure component parameters in the binary mixture model. For a simple case, it was proven that the quasi-chemical approximation would not predict the same energy for the pure component case and for a mixture of two identical components. However, the failure of the quasi-chemical approximation, does not explain the reason why the binary mixture model failed with the new set of parameters. The model failed, even with the new parameters because of numerous deviations of the real system from the assumptions of the lattice model. The lattice model proposed by Kamat et al., assume the adsorbate sites are highly localized. In actuality, the real system may have a larger accessible volume than permitted by the lattice model.

References

1. Kamat, Mithun and Keffer, David, "An analytical theory for diffusion of fluids in crystalline nanoporous materials", *MOL PHYS.* 2003 **101** p. 1399-1412.
2. Kamat, Mithun and Keffer, David, "A generalized analytical theory for adsorption of fluids in nanoporous materials", *MOL PHYS.* 2002 **100** p. 2689-2701.
3. Kamat, Mithun, Dang, W.J. and Keffer, David, "Agreement between analytical theory and molecular dynamics simulation for adsorption and diffusion in crystalline nanoporous materials", *J PHYS CHEM.* 2004 **108** p. 376-386.
4. Holister, Paul, Vas, Cristina Roman and Harper, Tim, "Technology White Papers nr.5", Cientifica Nanoporous Materials, www.cientifica.com, 2003.
5. ben-avraham, Daniel and Havlin, Shlomo, "Diffusion and Reactions in Fractals and Disordered Systems", New York: Cambirdge University Press, 2000.
6. Snurr, R.Q., June, R.L., Bell, A.T. and Theodorou, D.N., "Molecular simulations of methane adsorption in silicalite", *MOL SIM.* 1991 **8** p. 73-92.
7. Snurr, R.Q., June, R.L., Bell, A.T. and Theodorou, D.N., "A hierarchical atomistic/lattice simulation approach for the prediction of adsorption thermodynamics of benzene in silicalite", *J PHYS CHEM.* 1994 **98** p. 5111-5119.
8. Van Tassel, P.R., Somers, S.A., Davis, H. Ted and McCormick, Alon V., "Lattice model and simulation of dynamics of adsorbate motion in zeolites", *CHEM ENGR SCI.* 1994 **49** p. 2979-2989.
9. Van Tassel, P.R., Davis, H.T. and McCormick, A.V., "New lattice model for adsorption of small molecules and their mixtures in a zeolite micropore", *AICHE J.* 1994 **40** p. 925-934.
10. Van Tassel, P.R., Davis, H.T. and McCormick, A.V., "Adsorption simulations of small molecules and their mixtures in a zeolite micropore", *Langmuir.* 1994 **10** p. 1257-1267.
11. Grimmett, Geoffrey, "Percolation", Berlin: Springer, 1999.
12. Keffer, David., McCormick, Alon V. and Davis, H. Ted, "Diffusion and Percolation on Zeolite Sorption Lattices", *J PHYS CHEM.* 1996 **100** p. 967-973.
13. Kirkpatrick, Scott, "Percolation and Conduction", *REVIEWS OF MODERN PHYSICS.* 1973 **45** p. 574-588.
14. Saravanan, C. and Auerback, S.M., "Modeling the concentration dependence of diffusion in zeolites. I. Analytical theory of benezen in Na-Y", *J CHEM PHYS.* 1997 **107** p. 8120-8131.
15. Saravanan, C. and Auerback, S.M., "Modeling the concentration dependence of diffusion in zeolites. II. Kinetic Monte Carlo simulations of benzenein Na-Y", *J CHEM PHYS.* 1997 **107** p. 8131-8137.
16. Saravanan, C., Jousse, F. and Auerback, S.M., "Modeling the concentration dependence of diffusion in zeolites. III. Testing mean field theory for benzene in Na-Y with simulation", *J CHEM PHYS.* 1998 **108** p. 2162-2169.
17. Adhangale, Parag and Keffer, David, "A grand canonical Monte Carlo study of the adsorption of methane, ethane, and their mixtures in one-dimensional nanoporous materials", *Langmuir.* 2002 **18** p. 10455-10461.
18. Keffer, David, Gupta, V., Kim, D. and al., et, "A compendium of potential energy maps of zeolites and molecular sieves", *J MOL GRAPHICS.* 1996 **14** p. 108-&.

19. Hill, Terrell L., "Introduction to Statistical Thermodynamics", Mass.: Addison Wesley Pub. Co., 1960.
20. Gear, C.W., "The Numerical Integration of Ordinary Differential Equations of Various Orders", Argonne National Laboratory, ANL-7126, 1966.
21. Gear, C.W., "Numerical Initial Value Problems in Ordinary Differential Equations", Englewood Cliffs, New Jersey: Prentice Hall, Inc., 1971.
22. Allen, M.P. and Tildesly, D.J., "Computer Simulation of Liquids", Oxford: Oxford Science Publications, 1987.
23. Haile, J.M., "Molecular Dynamics Simulation", New York: John Wiley & Sons, Inc., 1992.
24. Software, Numerical Recipes, "Numerical Recipes Online", http://www.nr.com,
25. Adhangale, Parag and Keffer, David, "Exploiting single-file motion in one-dimensional nanoporous materials for hydrocarbon separation", *SEPAR SCI TECHNOL.* 2003 **38** p. 977-998.

Appendices

Appendix 1 – Nomenclature, Tables, and Figures for Part 2

Nomenclature

SYMBOL	DESCRIPTION	UNITS
p_i	Probability of a hop	-
D_i	Local self-diffusion coefficient	$\{m^2/s\}$
D_M	Mean self-diffusion coeffecient	$\{m^2/s\}$
$G(D)$	Bond conductances	-
δ	Dirac delta function	-
z	Connectivity of lattice	-
c_i	Coeffecient of polynomial	-
f_i	Function present in polynomial	-
$f_{2,i}$	Function present in polynomial	-
p	Probability of open bonds in a lattice	-
p_c	Percolation threshold	-

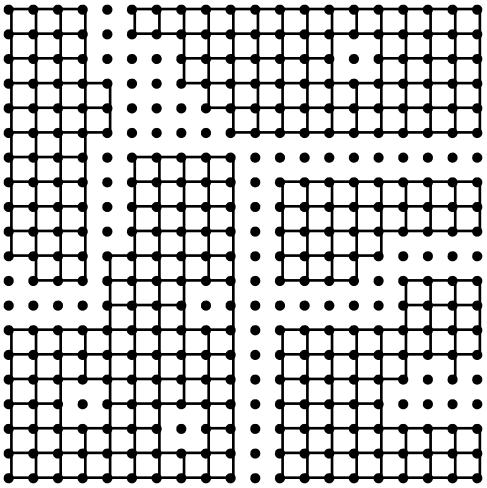

Figure (1): Percolation Lattice, $p<p_c$

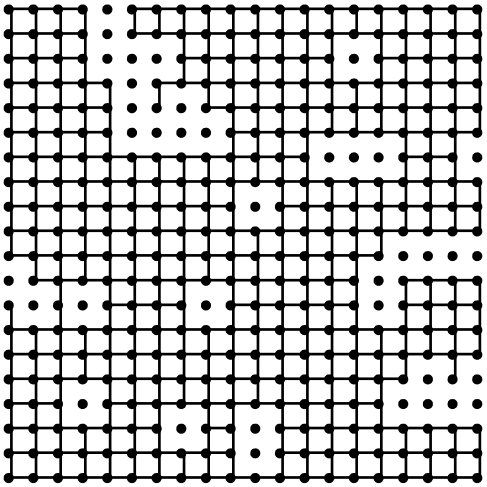

Figure (2): Percolation Lattice, $p>p_c$

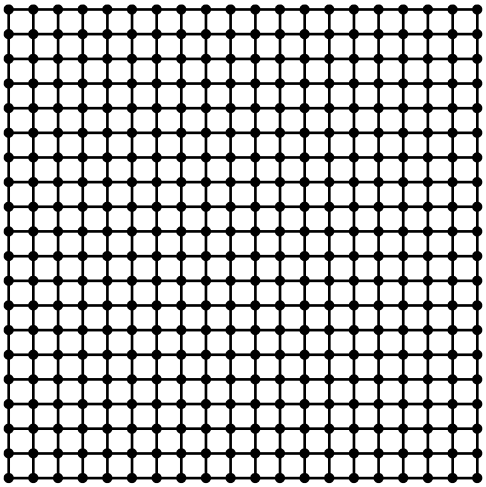

Figure (3): Percolation Lattice, $p=1$

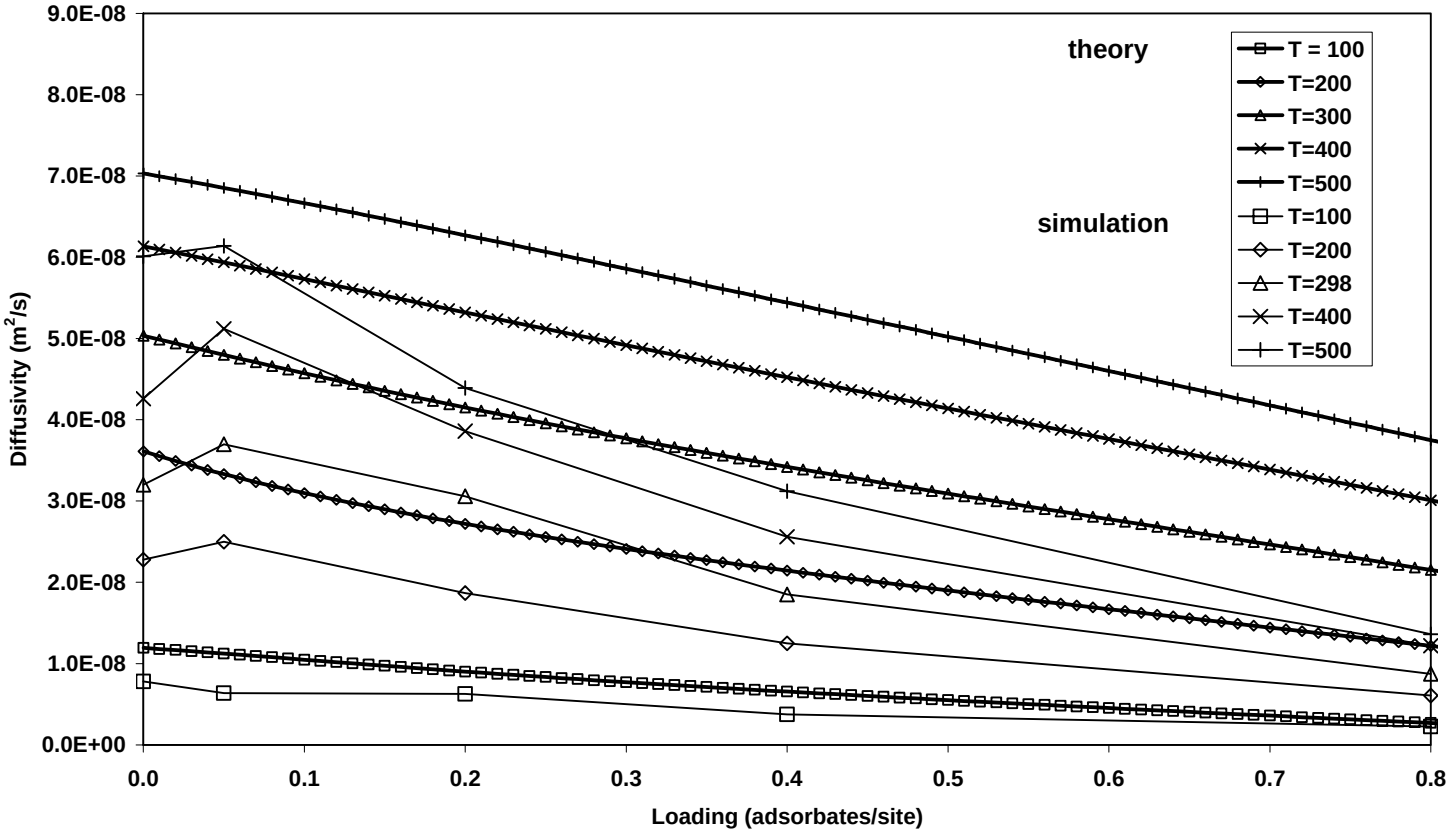

Figure (4): Methane self-diffusion coefficients

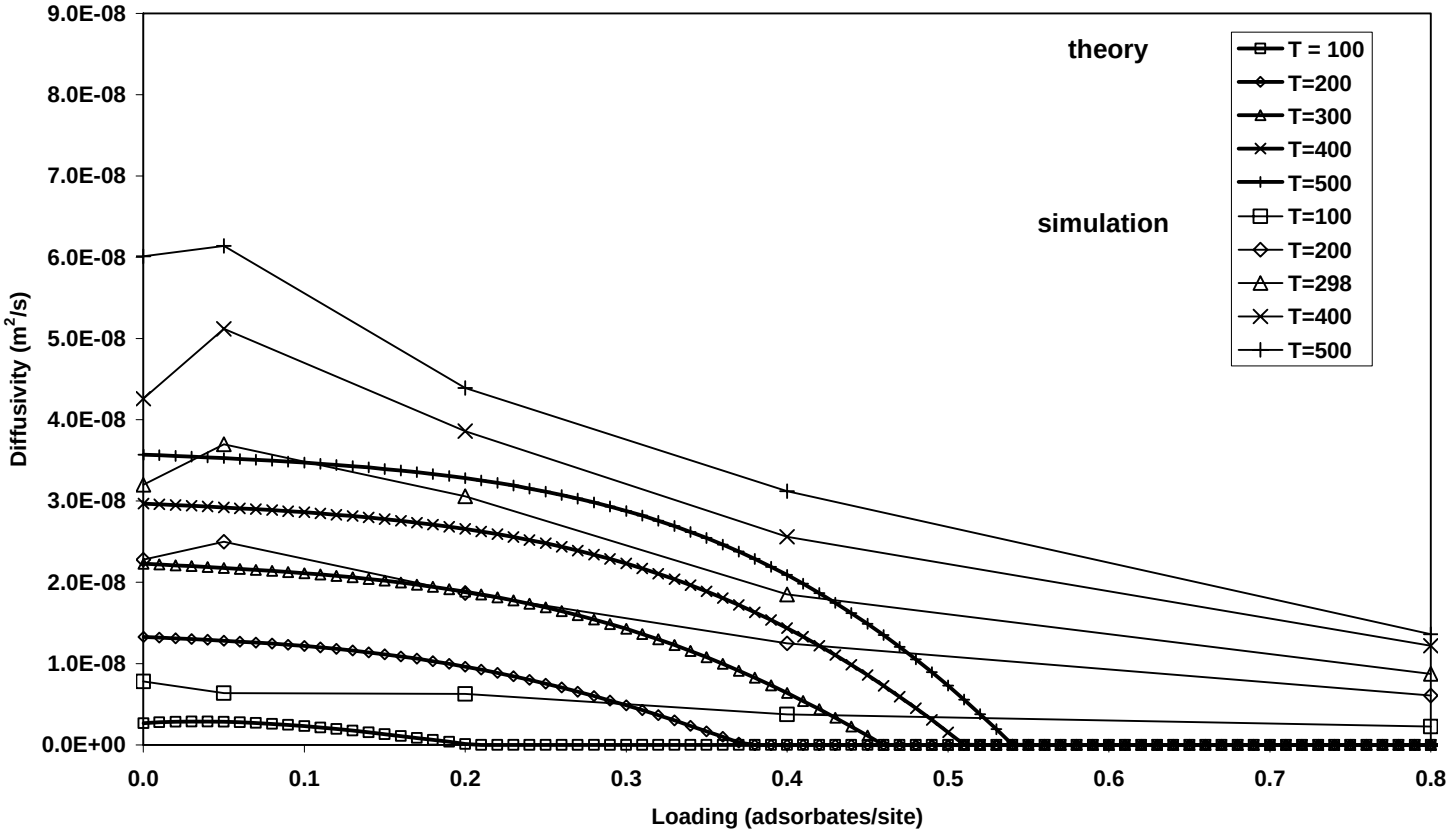

Figure (5): Methane self-diffusion coefficients with percolation

Appendix 2 – Nomenclature, Tables, and Figures for Part 3

Nomenclature

SYMBOL	DESCRIPTION	UNITS
c_{ij}	Number of sites of type *j* connected to a site of type *i*	-
$G(N,M)$	Configurational degeneracy of the lattice	-
k	Boltzmann constant	{J/mole/K}
$m_{s,i}$	Maximum occupancy of sites of type *i*	-
$n_{s,i}(x)$	Number of sites of type *i* with occupancy *x*	-
M	Number of sites	-
N	Number of adsorbates	-
$N_{ij,xy}$	Number of neighbors between sites of type *i* with occupancy *x* and sites of type *j* with occupancy *y*	-
$q_i(x,T)$	Intrasite partition function of sites of type *i*	-
$Q(N,M,T)$	Partition function of a function of N,M,T	-
$U_{AP,i}(x)$	Potential energy of a site of type *i* as a function of occupancy, *x*	{K/Molecule}
U_{AA}	Adsorbate-adsorbate interaction energy	{K/Molecule}
V_A	Volume of adsorbate	{Å^3}
$V_{S,i}$	Volume of sites of type *i*	{Å^3}
x	Occupancy of sites of type *i*	-
y	Occupancy of sites of type *j*	-
Λ	Thermal De Broglie Wavelength	{m}
$\underline{l}$	Matrix of distance between sites	{Å}
$U_{AP,i}(r,x)$	Adsorbate pore interaction energy as a function of site radius and the type of site.	{K/Molecule}
$U_{AP,i}(x)$	Adsorbate pore interaction energy as a function of the type of site.	{K/Molecule}
r_i	Radius of a site of type *i*	{Å}
$U_{APc,i}$	A fitting parameter for a site of type *i*.	{K/Molecule/ Å^2}
k_b	Boltzmann constant	{J/K}
T	Temperature	{K}
n	Number of data points in parameter optimization	
X_i	Data in objective function	
μ	Chemical potential	{kJ/mole}

Table 1. Summation indices

i	***j***	***x***	***y***
1	2	0	0
1	2	0	1
1	2	0	2
1	2	1	0
1	2	1	1
1	2	1	2

Table 2. Potential Parameters

	ε_{ij} / k {K}	σ_{ij} {Å}
methane – methane	3.882	81.97
ethane – ethane	4.418	137.62
methane – oxygen	3.083	84.41
ethane – oxygen	3.322	94.24

Table 3. Simulation Results – Methane in $AlPO_4$-5

Density	U_{ap}	U_{aa}	U_{TOT}	*Diff*	*T*
(adsorbates/site)	{K}	{K}	{K}	{m^2/sec}	{K}
0.13	-9.37E+02	-1.75E+01	-9.54E+02	2.66E-08	350
0.19	-9.44E+02	-2.78E+01	-9.72E+02	2.17E-08	
0.25	-9.50E+02	-3.77E+01	-9.88E+02	1.87E-08	
0.38	-9.64E+02	-5.77E+01	-1.02E+03	1.60E-08	
0.50	-9.78E+02	-7.75E+01	-1.06E+03	1.04E-08	
0.13	-9.15E+02	-1.61E+01	-9.31E+02	3.65E-08	400
0.19	-9.29E+02	-2.63E+01	-9.56E+02	3.01E-08	
0.25	-9.33E+02	-3.61E+01	-9.70E+02	2.15E-08	
0.38	-9.44E+02	-5.44E+01	-9.98E+02	1.83E-08	
0.50	-9.57E+02	-7.36E+01	-1.03E+03	1.43E-08	
0.13	-9.03E+02	-1.63E+01	-9.19E+02	3.88E-08	450
0.19	-9.13E+02	-2.46E+01	-9.38E+02	2.83E-08	
0.25	-9.19E+02	-3.41E+01	-9.53E+02	2.05E-08	
0.38	-9.27E+02	-5.11E+01	-9.78E+02	1.86E-08	
0.50	-9.46E+02	-7.09E+01	-1.02E+03	1.40E-08	
0.13	-9.00E+02	-1.61E+01	-9.16E+02	3.55E-08	500
0.19	-9.00E+02	-2.44E+01	-9.25E+02	3.07E-08	
0.25	-9.06E+02	-3.20E+01	-9.38E+02	2.52E-08	
0.38	-9.20E+02	-4.97E+01	-9.70E+02	1.93E-08	
0.50	-9.27E+02	-6.58E+01	-9.93E+02	1.72E-08	
0.13	-8.84E+02	-1.40E+01	-8.98E+02	4.09E-08	550
0.19	-8.91E+02	-2.28E+01	-9.14E+02	3.41E-08	
0.25	-8.96E+02	-3.10E+01	-9.27E+02	2.75E-08	
0.38	-9.04E+02	-4.70E+01	-9.51E+02	2.51E-08	
0.50	-9.19E+02	-6.36E+01	-9.83E+02	1.90E-08	
0.13	-8.70E+02	-1.38E+01	-8.84E+02	5.55E-08	600
0.19	-8.77E+02	-2.13E+01	-8.98E+02	3.18E-08	
0.25	-8.83E+02	-2.91E+01	-9.12E+02	3.05E-08	
0.38	-8.92E+02	-4.39E+01	-9.36E+02	2.10E-08	
0.50	-9.06E+02	-6.03E+01	-9.67E+02	2.01E-08	

Table 4. Simulation Results – Ethane in $AlPO_4$-5

Density	U_{ap}	U_{aa}	U_{TOT}	*Diff*	*T*
adsorbates/site	{K}	{K}	{K}	{m^2/sec}	{K}
0.13	-1.83E+03	-4.30E+01	-1.87E+03	1.27E-08	350
0.19	-1.85E+03	-7.15E+01	-1.93E+03	1.02E-08	
0.25	-1.86E+03	-9.23E+01	-1.95E+03	8.93E-09	
0.38	-1.89E+03	-1.44E+02	-2.04E+03	6.73E-09	
0.50	-1.93E+03	-1.99E+02	-2.12E+03	4.82E-09	
0.13	-1.79E+03	-4.11E+01	-1.84E+03	1.66E-08	400
0.19	-1.81E+03	-6.52E+01	-1.87E+03	1.00E-08	
0.25	-1.81E+03	-8.49E+01	-1.89E+03	1.08E-08	
0.38	-1.84E+03	-1.33E+02	-1.97E+03	6.65E-09	
0.50	-1.89E+03	-1.91E+02	-2.09E+03	4.95E-09	
0.13	-1.75E+03	-3.91E+01	-1.79E+03	1.74E-08	450
0.19	-1.76E+03	-5.91E+01	-1.82E+03	1.41E-08	
0.25	-1.78E+03	-7.87E+01	-1.86E+03	9.20E-09	
0.38	-1.82E+03	-1.32E+02	-1.96E+03	6.23E-09	
0.50	-1.86E+03	-1.81E+02	-2.04E+03	6.26E-09	
0.13	-1.72E+03	-3.66E+01	-1.76E+03	1.50E-08	500
0.19	-1.74E+03	-5.82E+01	-1.80E+03	1.26E-08	
0.25	-1.74E+03	-7.63E+01	-1.82E+03	9.87E-09	
0.38	-1.79E+03	-1.24E+02	-1.91E+03	6.23E-09	
0.50	-1.82E+03	-1.74E+02	-2.00E+03	7.55E-09	
0.13	-1.70E+03	-3.48E+01	-1.73E+03	1.88E-08	550
0.19	-1.72E+03	-5.38E+01	-1.77E+03	1.01E-08	
0.25	-1.73E+03	-7.46E+01	-1.80E+03	8.94E-09	
0.38	-1.76E+03	-1.18E+02	-1.88E+03	7.75E-09	
0.50	-1.80E+03	-1.66E+02	-1.96E+03	5.99E-09	
0.13	-1.68E+03	-3.38E+01	-1.71E+03	1.50E-08	600
0.19	-1.69E+03	-5.04E+01	-1.74E+03	1.36E-08	
0.25	-1.70E+03	-6.92E+01	-1.77E+03	1.21E-08	
0.38	-1.74E+03	-1.16E+02	-1.86E+03	9.68E-09	
0.50	-1.77E+03	-1.59E+02	-1.93E+03	7.52E-09	

Table 5. Lattice Parameters – Methane

N_T=2, $\underline{m_s}$= [1 2]

$\underline{c}$	$\underline{l}$ (Å)	$\underline{V_s}$ (Å^3)	$\underline{U_{ap}}$ (K)	$\underline{U_{apc}}$ (K)
$\begin{bmatrix} 0 & 2 \\ 2 & 0 \end{bmatrix}$	$\begin{bmatrix} - & 3.59 \\ 3.59 & - \end{bmatrix}$	$\begin{bmatrix} 64.37 & 115.63 \end{bmatrix}$	$\begin{bmatrix} -302.62 & -1266.95 \\ - & -1266.95 \end{bmatrix}$	$\begin{bmatrix} 0 & 650 \\ 0 & 650 \end{bmatrix}$

Table 6. Lattice Parameters – Ethane

N_T=2, $\underline{m_s}$= [1 2]

$\underline{c}$	$\underline{l}$ (Å)	$\underline{V_s}$ (Å^3)	$\underline{U_{ap}}$ (K)	$\underline{U_{apc}}$ (K)
$\begin{bmatrix} 0 & 2 \\ 2 & 0 \end{bmatrix}$	$\begin{bmatrix} - & 4.07 \\ 4.07 & - \end{bmatrix}$	$\begin{bmatrix} 87.00 & 93.00 \end{bmatrix}$	$\begin{bmatrix} -1181.68 & -2297.98 \\ - & -2297.98 \end{bmatrix}$	$\begin{bmatrix} 0 & 1083.41 \\ 0 & 1083.41 \end{bmatrix}$

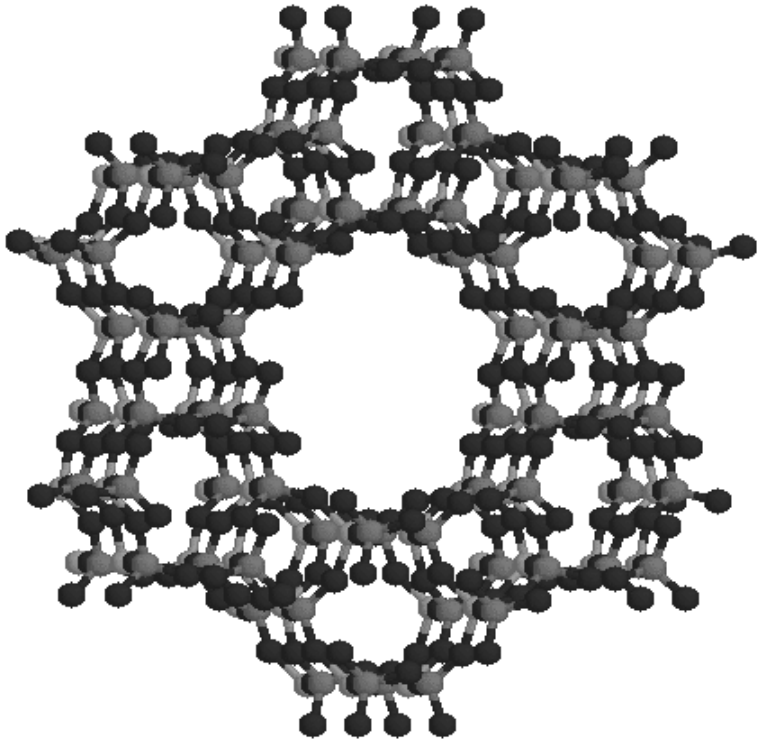

Figure (1): Schematic of the $AlPO_4$-5 structure

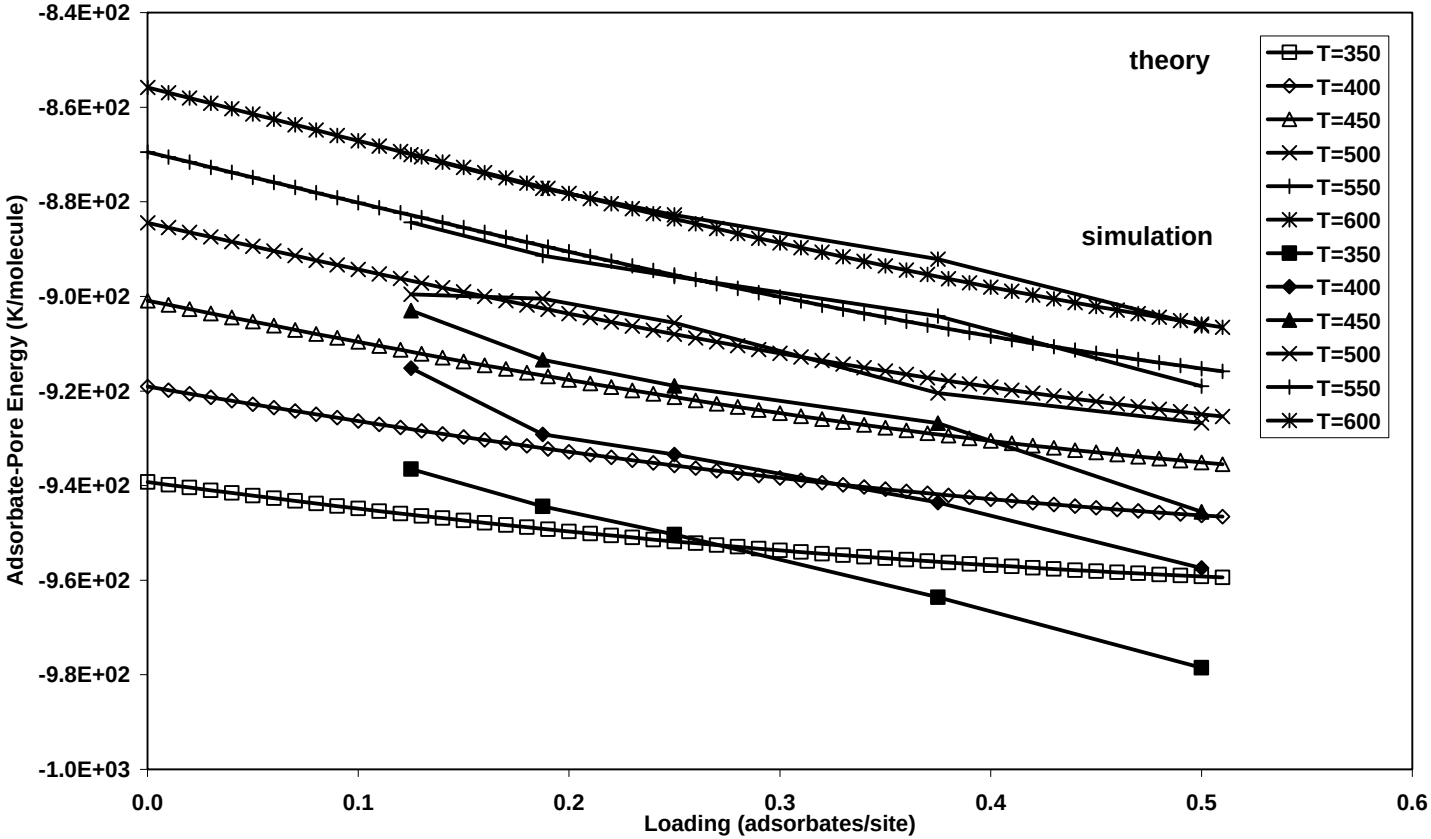

Figure (2): Methane adsorbate-pore interaction energy as a function of fractional occupancy

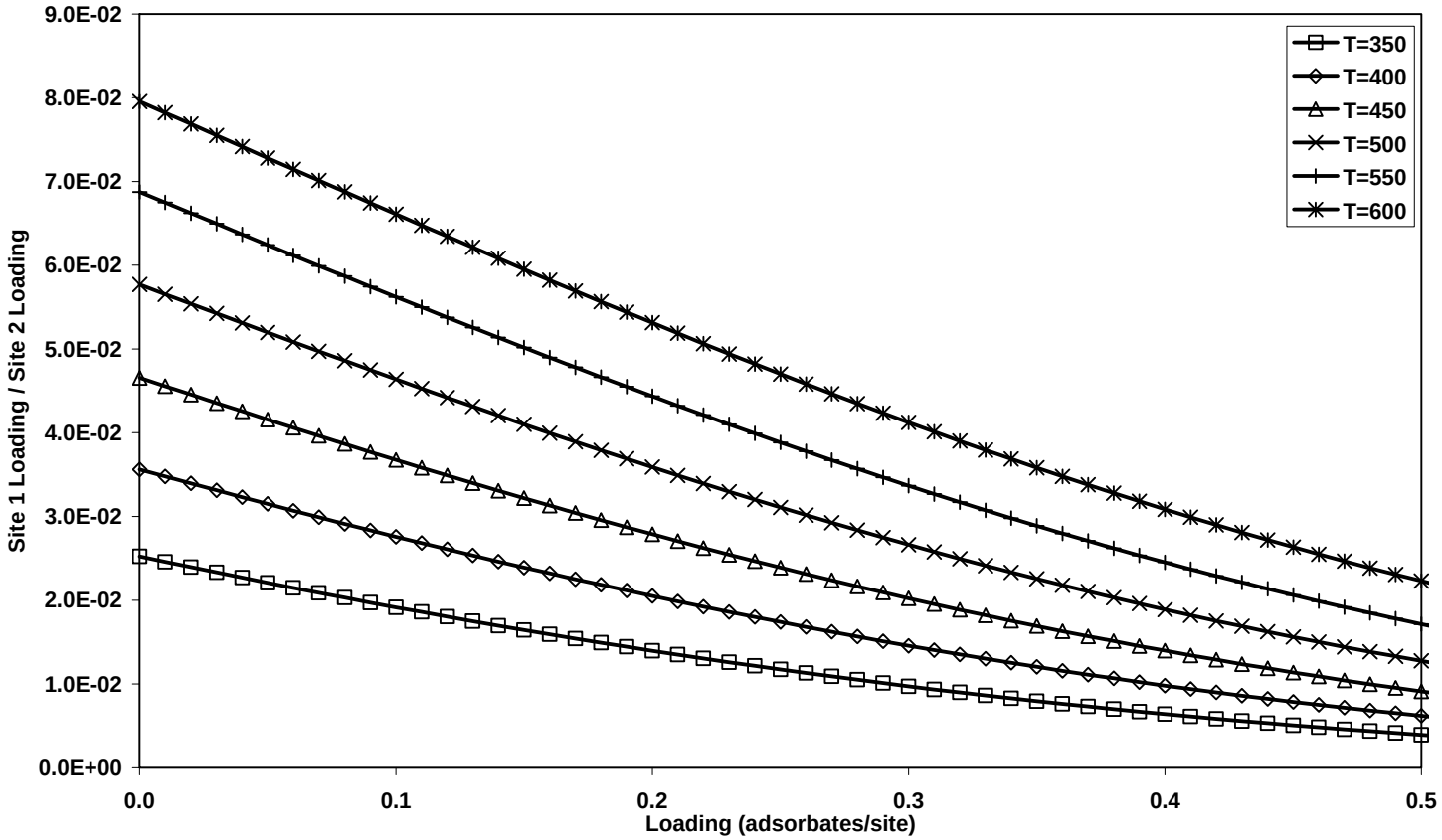

Figure (3): Methane adsorbate distribution versus adsorbate density

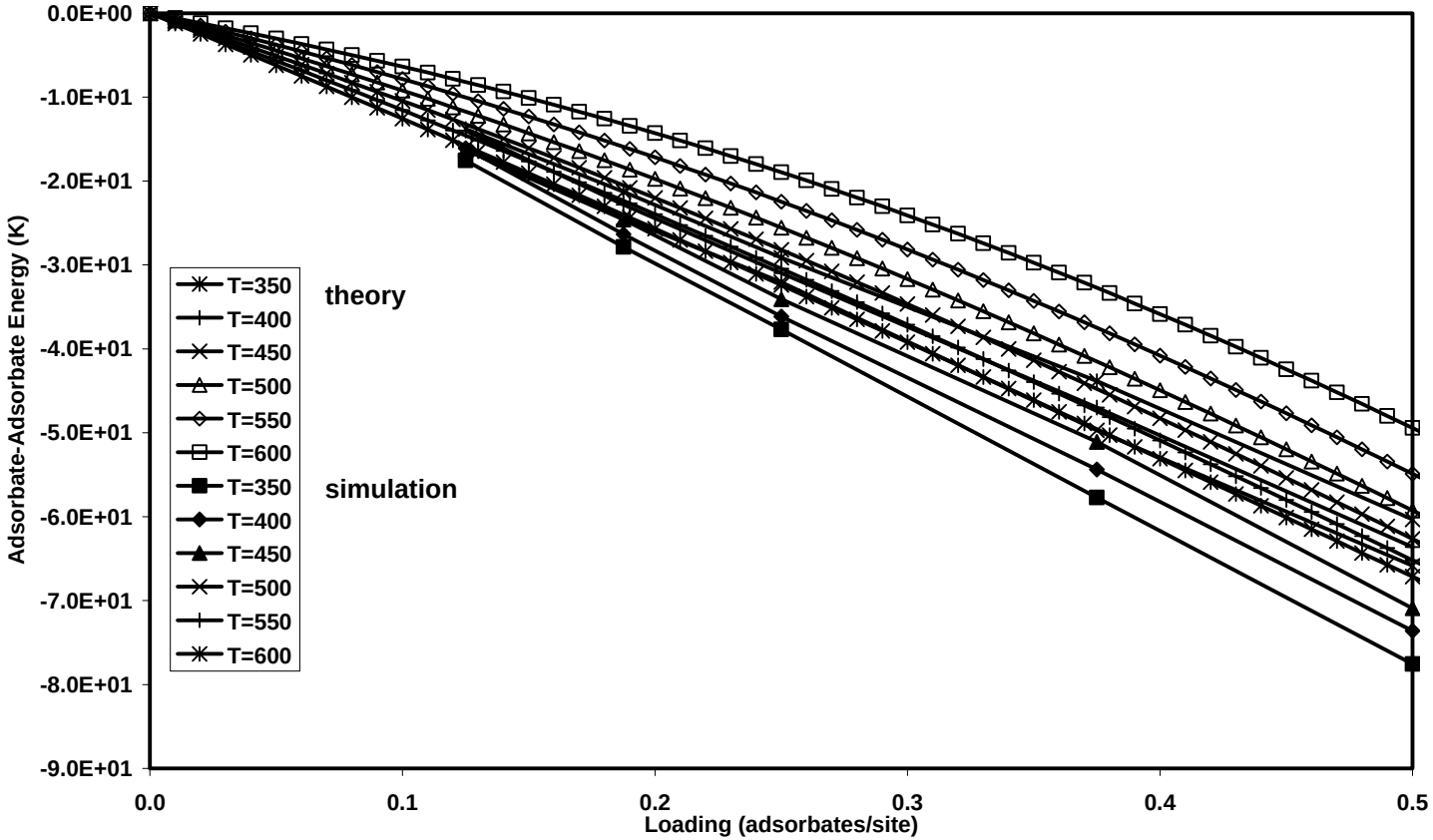

Figure (4): Methane adsorbate-adsorbate interaction energy as a function of fractional occupancy

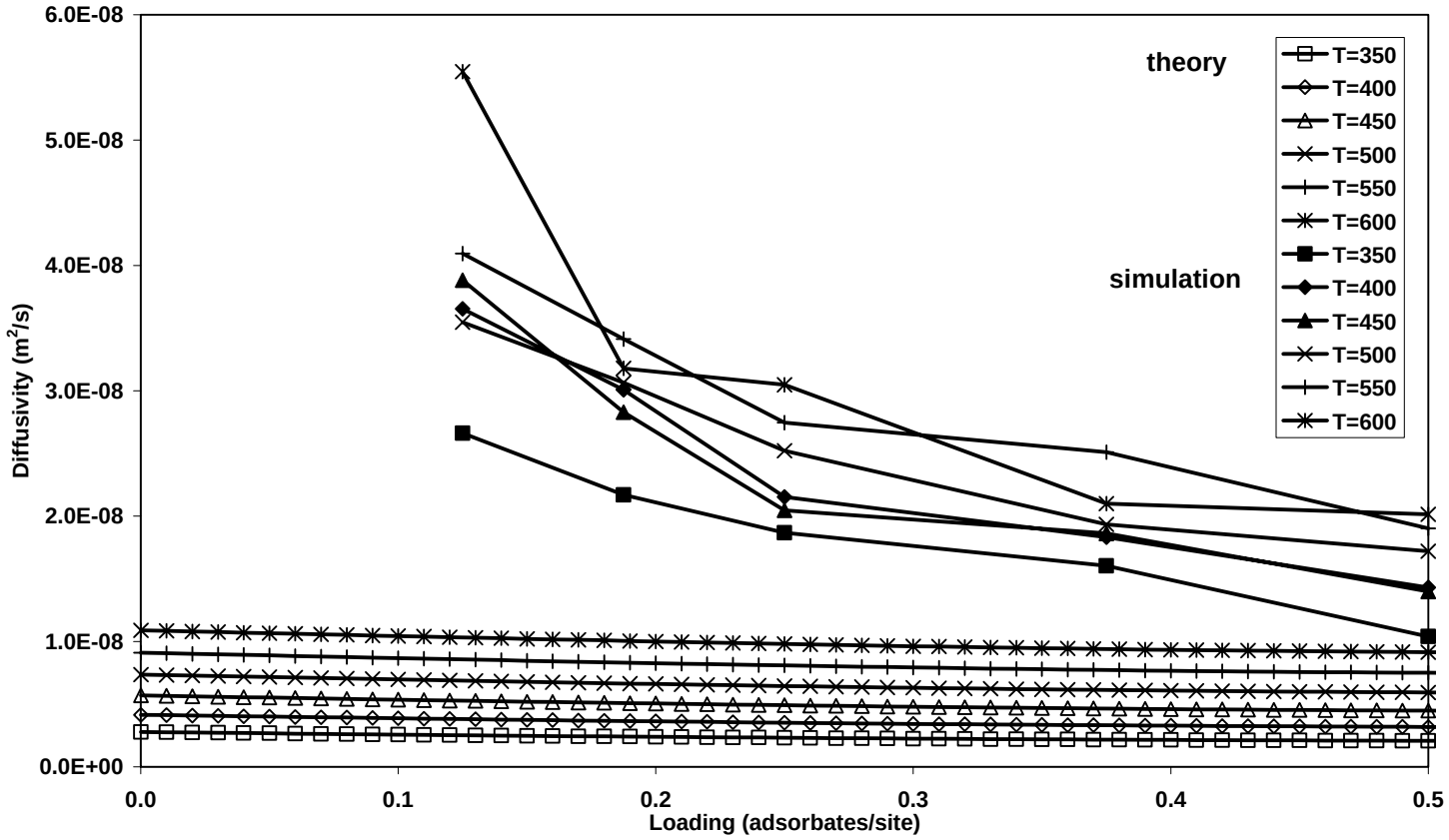

Figure (5): Methane self-diffusion coefficients as a function of fractional occupancy

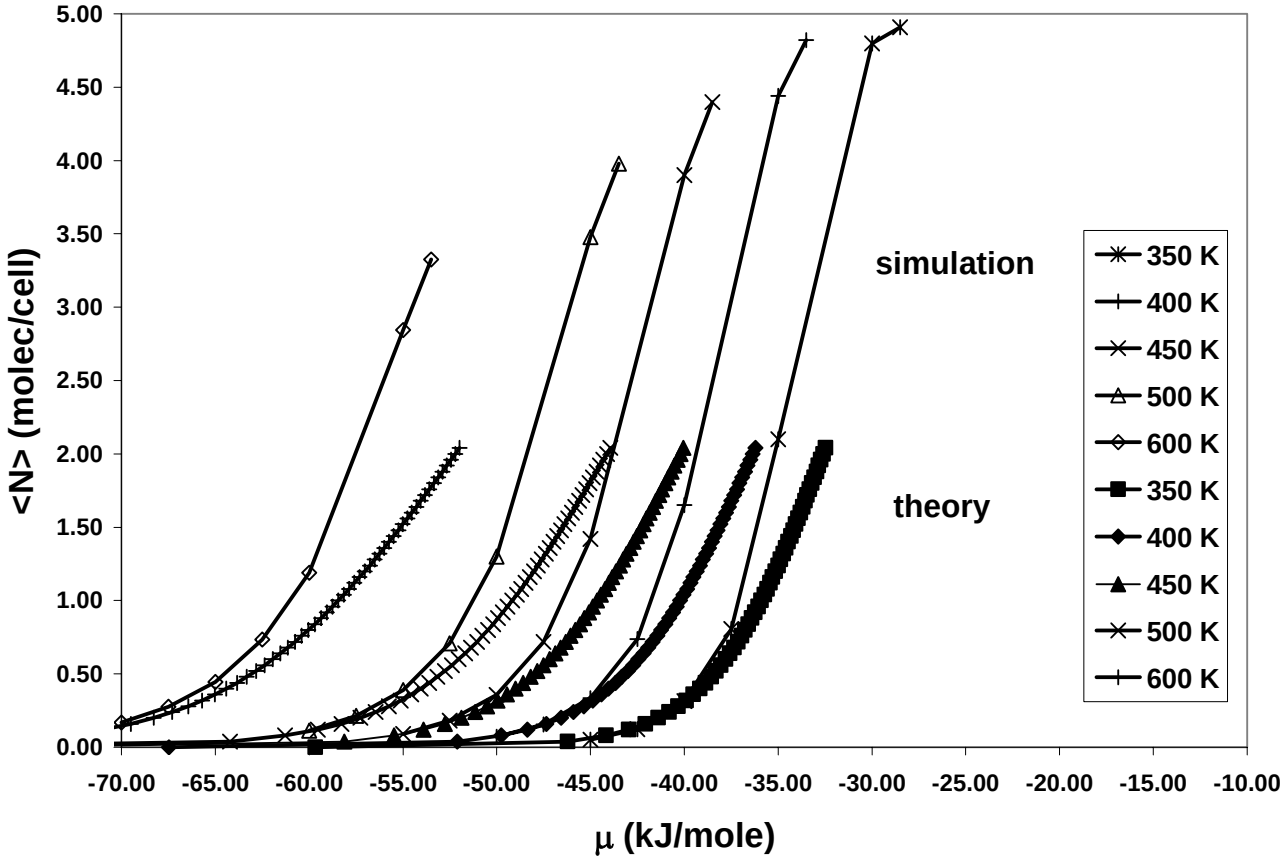

Figure (6): Methane adsorption isotherms

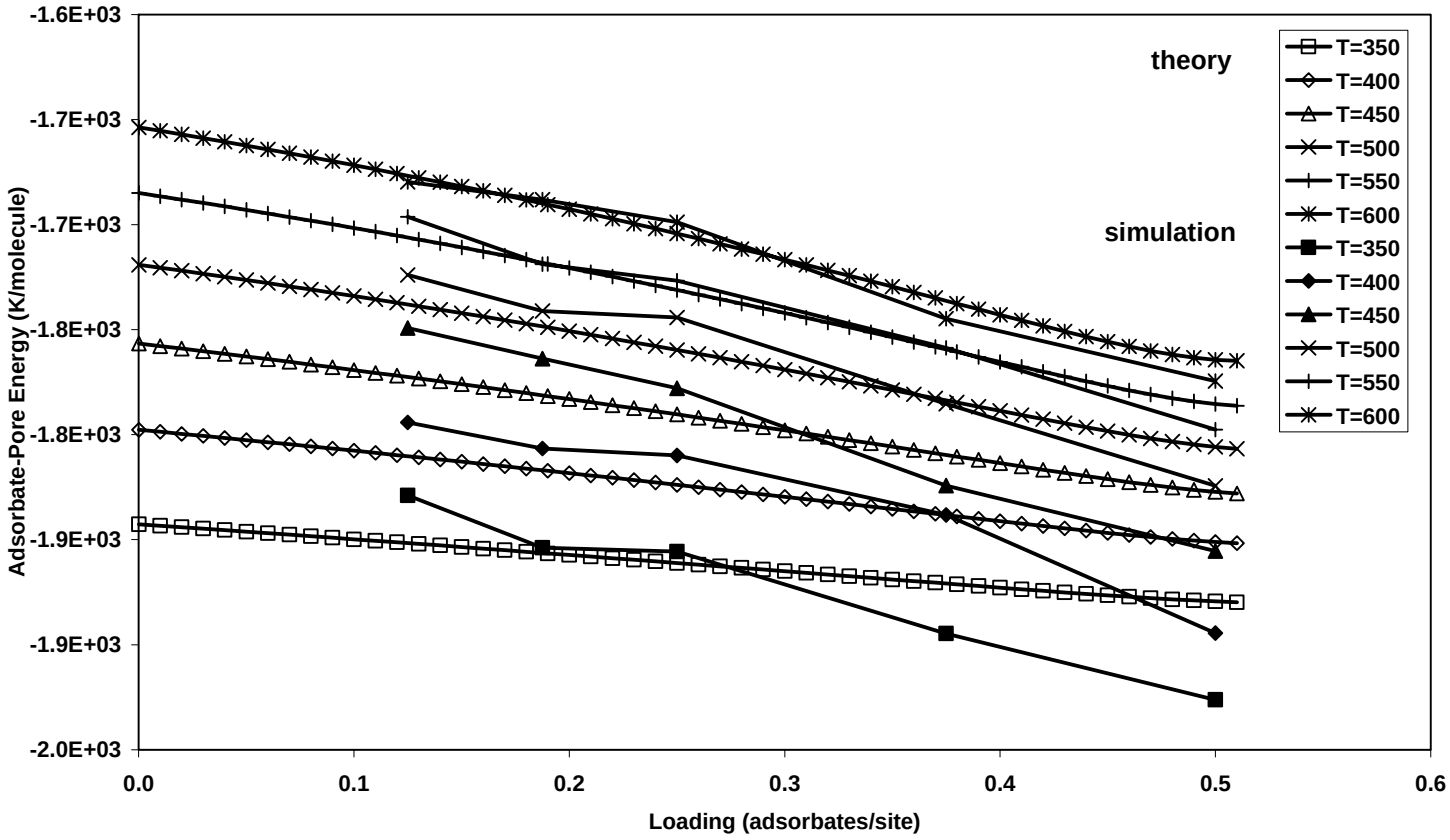

Figure (7): Ethane adsorbate-pore interaction energy as a function of fractional occupancy

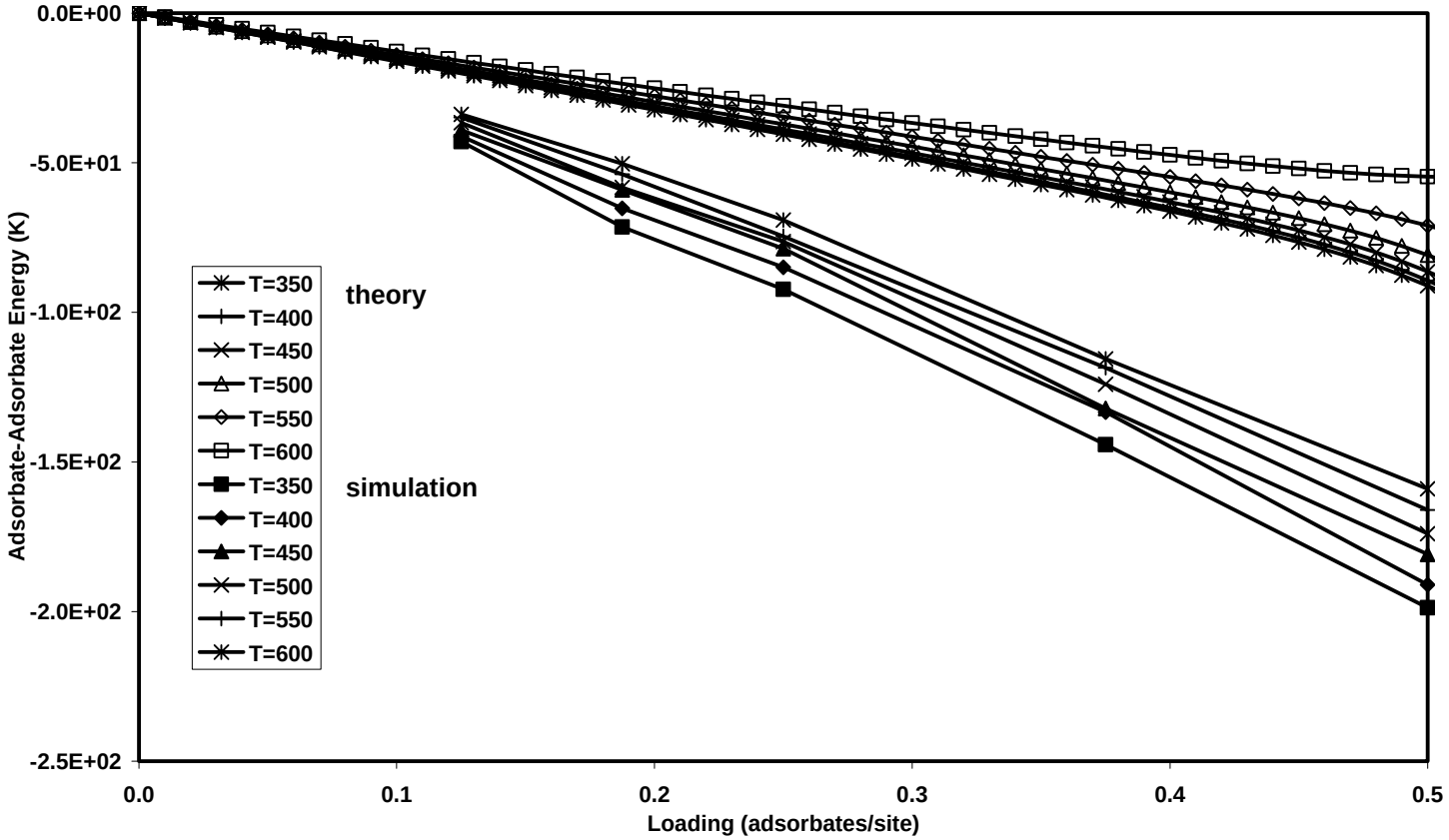

Figure (8): Ethane adsorbate-adsorbate interaction energy as a function of fractional occupancy

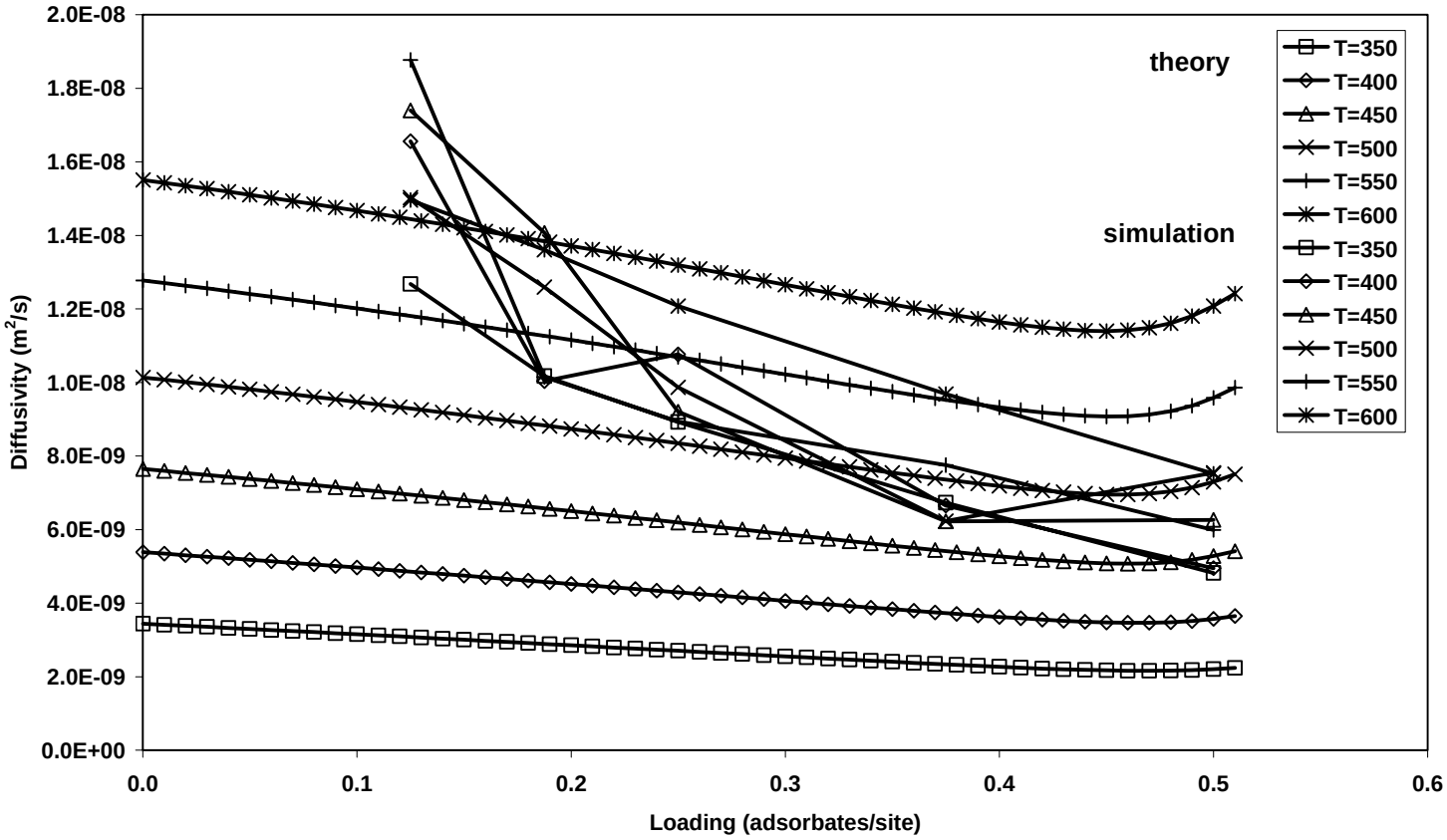

Figure (9): Ethane self-diffusion coefficients as a function of fractional occupancy

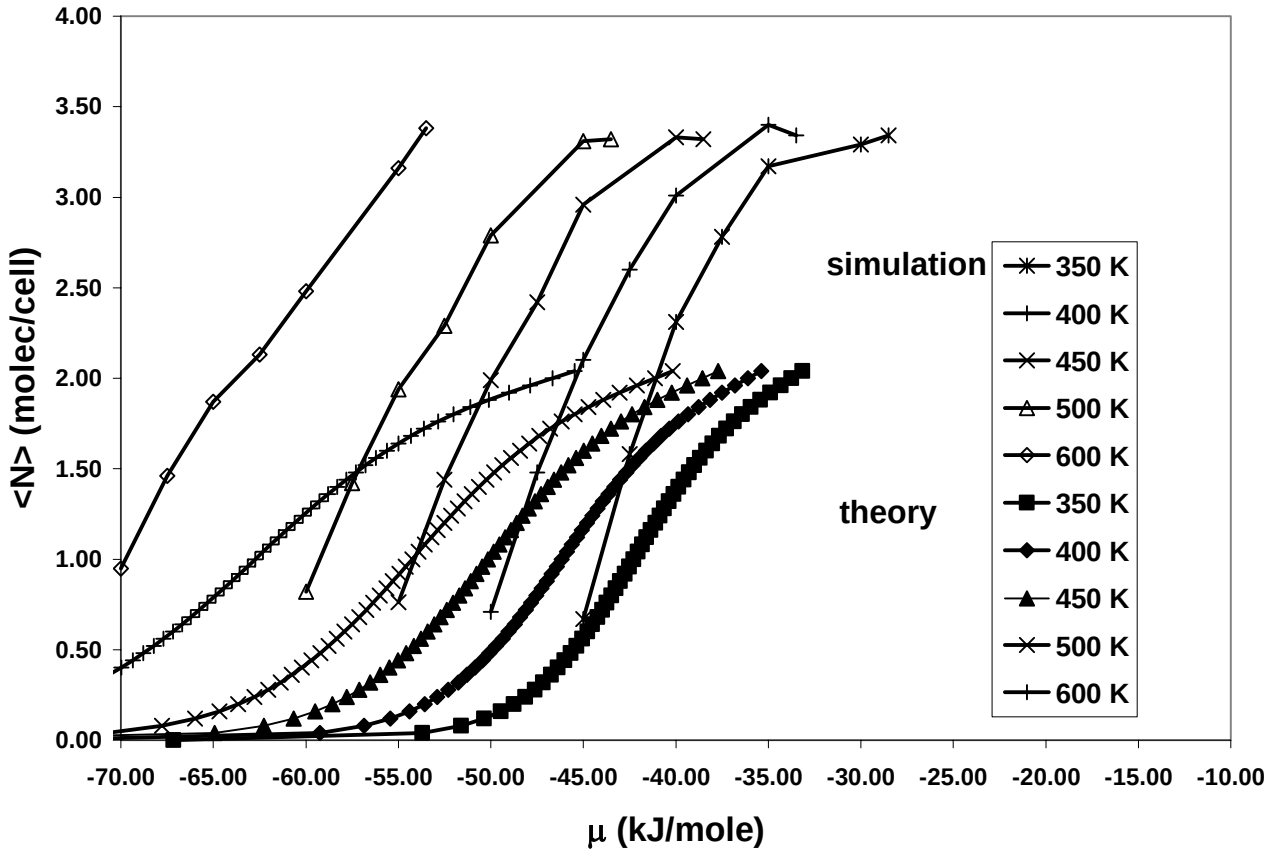

Figure (10): Ethane adsorption isotherms

Appendix 3 – Nomenclature, Tables, and Figures for Part 4

Nomenclature

SYMBOL	DESCRIPTION	UNITS
$g(N_1,N_2,M)$	Configurational degeneracy of the lattice for a binary mixture	-
k	Boltzmann constant	{J/mole/K}
$m_{s,i}$	Maximum occupancy of sites of type i	-
$n_{s,i}(x,y)$	Number of sites of type i with occupancy x of component 1 and occupancy y of component 2	-
M	Number of sites	-
N_i	Number of adsorbates of type i	-
$N_{ij}(x,y,w,z)$	Number of neighbors between sites of type i with occupancy x of component 1 and occupancy y of component 2 and sites of type j with occupancy w of component 1 and occupancy z of component 2	-
$q_{i,j}(x,y,T)$	Intrasite partition function of sites of type I for adsorbed component j	-
$Q(N_1,N_2,M,T)$	Partition function	-
$V_A(x)$	Volume of adsorbate of type x	{Å^3}
$V_{s,i}$	Volume of sites of type i	{Å^3}
x	Occupancy of sites of type i	-
y	Occupancy of sites of type j	-
Λ	Thermal De Broglie Wavelength	{m}
$qterm$	Intrasite partition function	-
$eterm$	Intersite interaction energy	{K/Molecule}
$w_i(k,m)$	Interaction energy of sites of type i with k occupancy of component 1, and m occupancy of component 2	{K}
σ_{MIX}	Lennard-Jones potential parameter	{K}
ε_{MIX}	Lennard-Jones potential parameter	{Å}
g	Configurational degeneracy for example case	-
$n_s(x)$	Number of sites with occupancy x (single component)	-
$n_s(A)$	Number of sites occupied by component A (binary mixture model)	-
N_{xy}	Number of sites with occupancy x neighboring a site with occupancy y (single component model)	-
N_{AB}	Number of sites occupied by component A neighboring a site occupied by component B (binary mixture model)	-
l_{mix}	Separation distance for Me-Et interactions	{Å}
V_{acc}	Accessible volume for half of a unit cell	

Table 1. Simulation Results – Binary Mixture

Density	*Uap*	*Uaa*	*Utot*	*Diff - Meth*	*Diff - Eth*	*T*
adsorbates/site	{K}	{K}	{K}	{m2/sec}	{m2/sec}	{K}
0.13	-1.40E+03	-3.08E+01	-1.43E+03	2.88E-08	1.46E-08	350
0.19	-1.40E+03	-4.80E+01	-1.45E+03	1.93E-08	1.27E-08	
0.25	-1.40E+03	-6.28E+01	-1.47E+03	1.70E-08	1.04E-08	
0.38	-1.43E+03	-9.56E+01	-1.52E+03	1.14E-08	7.89E-09	
0.50	-1.45E+03	-1.30E+02	-1.58E+03	9.28E-09	5.17E-09	
0.13	-1.35E+03	-2.82E+01	-1.38E+03	2.83E-08	1.57E-08	400
0.19	-1.36E+03	-4.31E+01	-1.40E+03	2.43E-08	1.43E-08	
0.25	-1.37E+03	-5.92E+01	-1.43E+03	2.23E-08	1.09E-08	
0.38	-1.40E+03	-8.97E+01	-1.49E+03	1.02E-08	8.25E-09	
0.50	-1.43E+03	-1.24E+02	-1.55E+03	9.28E-09	5.45E-09	
0.13	-1.34E+03	-2.62E+01	-1.36E+03	3.00E-08	1.73E-08	450
0.19	-1.34E+03	-4.00E+01	-1.38E+03	2.59E-08	1.39E-08	
0.25	-1.35E+03	-5.49E+01	-1.41E+03	2.33E-08	1.03E-08	
0.38	-1.37E+03	-8.44E+01	-1.45E+03	1.46E-08	9.27E-09	
0.50	-1.39E+03	-1.18E+02	-1.51E+03	9.76E-09	7.52E-09	
0.13	-1.31E+03	-2.38E+01	-1.33E+03	3.23E-08	1.38E-08	500
0.19	-1.31E+03	-3.75E+01	-1.35E+03	2.67E-08	1.20E-08	
0.25	-1.33E+03	-5.21E+01	-1.38E+03	2.14E-08	1.11E-08	
0.38	-1.36E+03	-8.33E+01	-1.44E+03	1.31E-08	9.26E-09	
0.50	-1.38E+03	-1.16E+02	-1.50E+03	9.79E-09	8.54E-09	
0.13	-1.30E+03	-2.32E+01	-1.32E+03	4.06E-08	1.95E-08	550
0.19	-1.30E+03	-3.62E+01	-1.34E+03	3.15E-08	1.52E-08	
0.25	-1.31E+03	-5.00E+01	-1.36E+03	2.70E-08	1.37E-08	
0.38	-1.33E+03	-7.81E+01	-1.41E+03	1.64E-08	1.29E-08	
0.50	-1.36E+03	-1.08E+02	-1.46E+03	1.33E-08	8.01E-09	
0.13	-1272.8347	-22.473003	-1295.3056	3.4251E-08	2.2291E-08	600
0.19	-1289.7355	-35.368679	-1325.1065	2.7409E-08	1.4805E-08	
0.25	-1294.7935	-47.365463	-1342.1573	2.915E-08	1.5441E-08	
0.38	-1312.4912	-74.265856	-1386.7567	1.6131E-08	1.1148E-08	
0.50	-1334.7499	-102.10796	-1436.8593	1.4891E-08	8.4682E-09	

Table 2. Lattice Parameters – Simultaneous optimization, Connectivity and Volume

N_T=2, $\underline{m}_s$= [1 2]

C	$\underline{V}_s$ (Å^3)
$\begin{bmatrix} 0 & 2 \\ 2 & 0 \end{bmatrix}$	$\begin{bmatrix} 82.00 & 98.00 \end{bmatrix}$

Table 3. Lattice Parameters – Simultaneous optimization, Separation Distance, Well Depth, and Well Steepness

N_T=2, $\underline{m}_s$= [1 2]

Species	$\underline{l}$ (Å)	$\underline{U}_{ap}$ (K)	$\underline{U}_{apc}$ (K)
Methane	$\begin{bmatrix} - & 3.57 \\ 3.57 & - \end{bmatrix}$	$\begin{bmatrix} -602.31 & -1251.04 \\ - & -1251.04 \end{bmatrix}$	$\begin{bmatrix} 0 & 529.78 \\ - & 529.78 \end{bmatrix}$
Ethane	$\begin{bmatrix} - & 4.11 \\ 4.11 & - \end{bmatrix}$	$\begin{bmatrix} -1097.21 & -2234.66 \\ - & -2234.66 \end{bmatrix}$	$\begin{bmatrix} 0 & 900.00 \\ - & 900.00 \end{bmatrix}$

Table 4. Lattice Parameters – Re-optimized parameters, Connectivity and Volume

N_T=2, $\underline{m}_s$= [1 2]

c	$\underline{V}_s$ (Å^3)
$\begin{bmatrix} 0 & 2 \\ 2 & 0 \end{bmatrix}$	$\begin{bmatrix} 49.85 & 130.15 \end{bmatrix}$

Table 5. Lattice Parameters – Re-optimized parameters, Separation Distance, Well Depth, and Well Steepness

N_T=2, $\underline{m_s}$= [1 2]

Species	$\underline{l}$ (Å)	$\underline{U_{ap}}$ (K)	$\underline{U_{apc}}$ (K)
Methane	$\begin{bmatrix} - & 4.97 \\ 4.97 & - \end{bmatrix}$	$\begin{bmatrix} -719.46 & -1113.17 \\ - & -1113.17 \end{bmatrix}$	$\begin{bmatrix} 0 & 230.89 \\ - & 230.89 \end{bmatrix}$
Ethane	$\begin{bmatrix} - & 4.47 \\ 4.47 & - \end{bmatrix}$	$\begin{bmatrix} -800.36 & -2234.84 \\ - & -2234.84 \end{bmatrix}$	$\begin{bmatrix} 0 & 1045.53 \\ - & 1045.53 \end{bmatrix}$

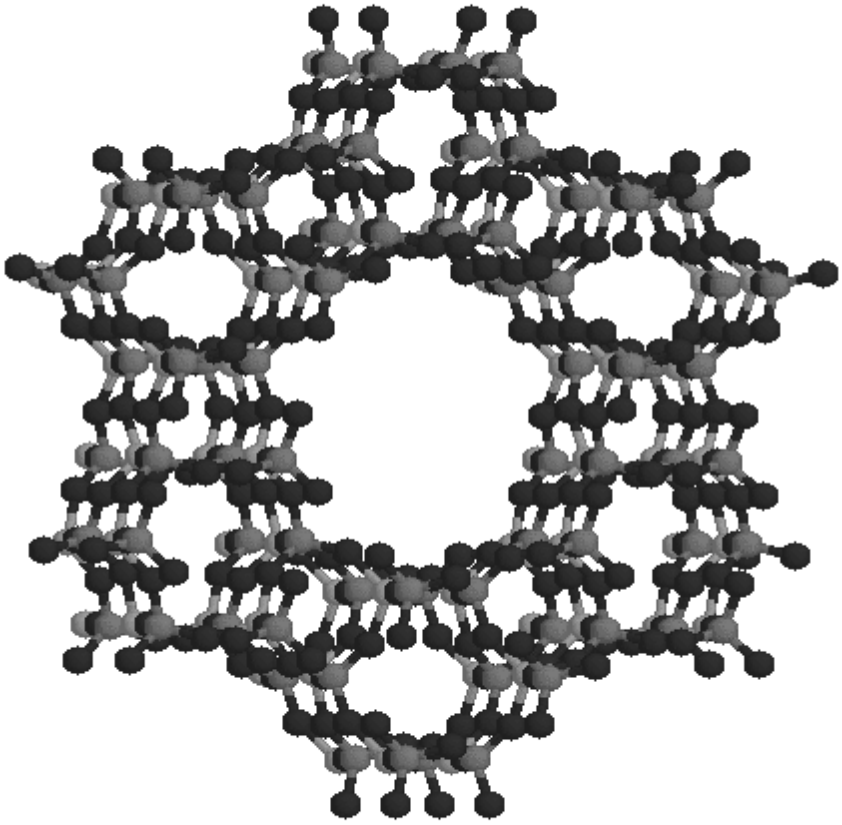

Figure (1): Schematic of the $AlPO_4$-5 structure

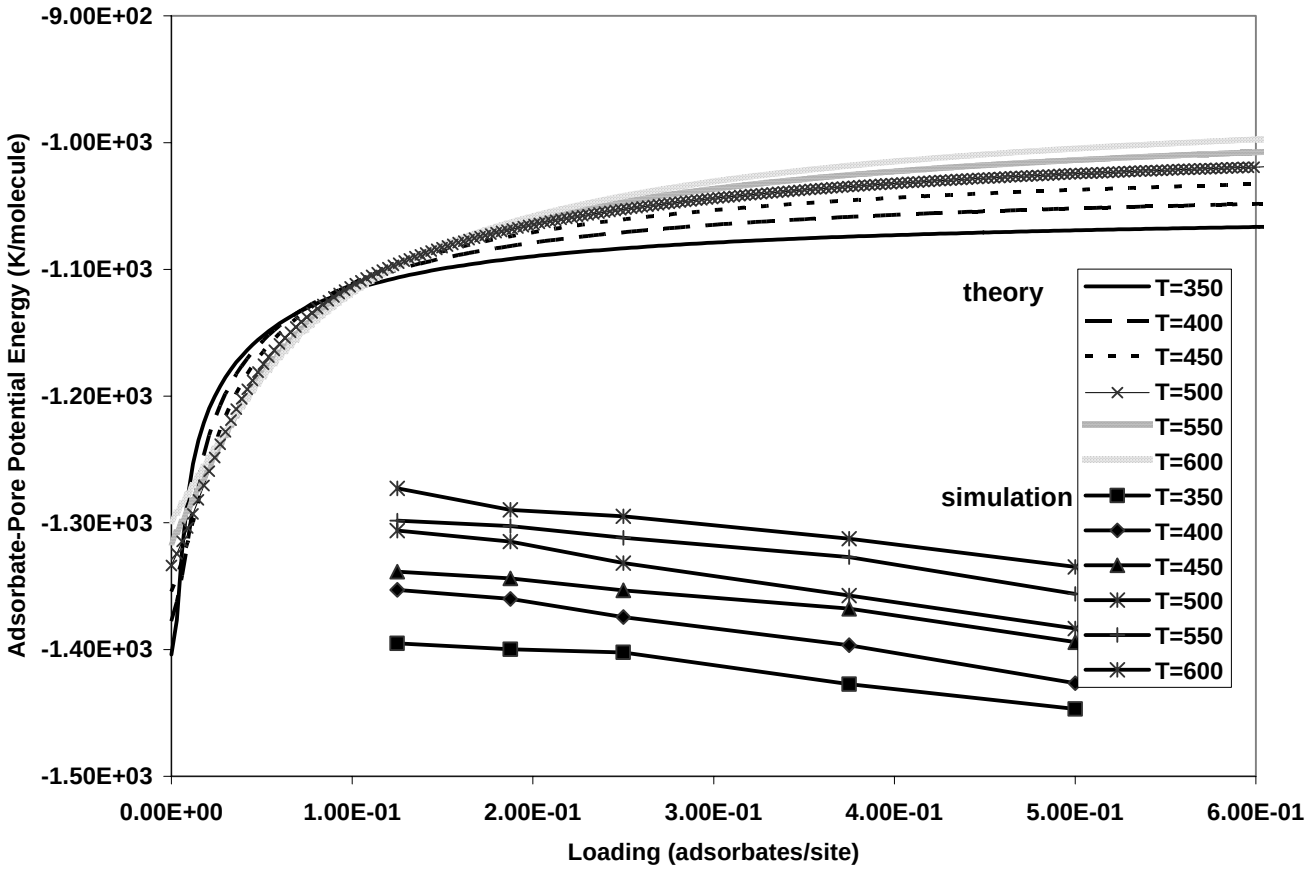

Figure (2): Adsorbate-pore interaction energy as a function of fractional occupancy

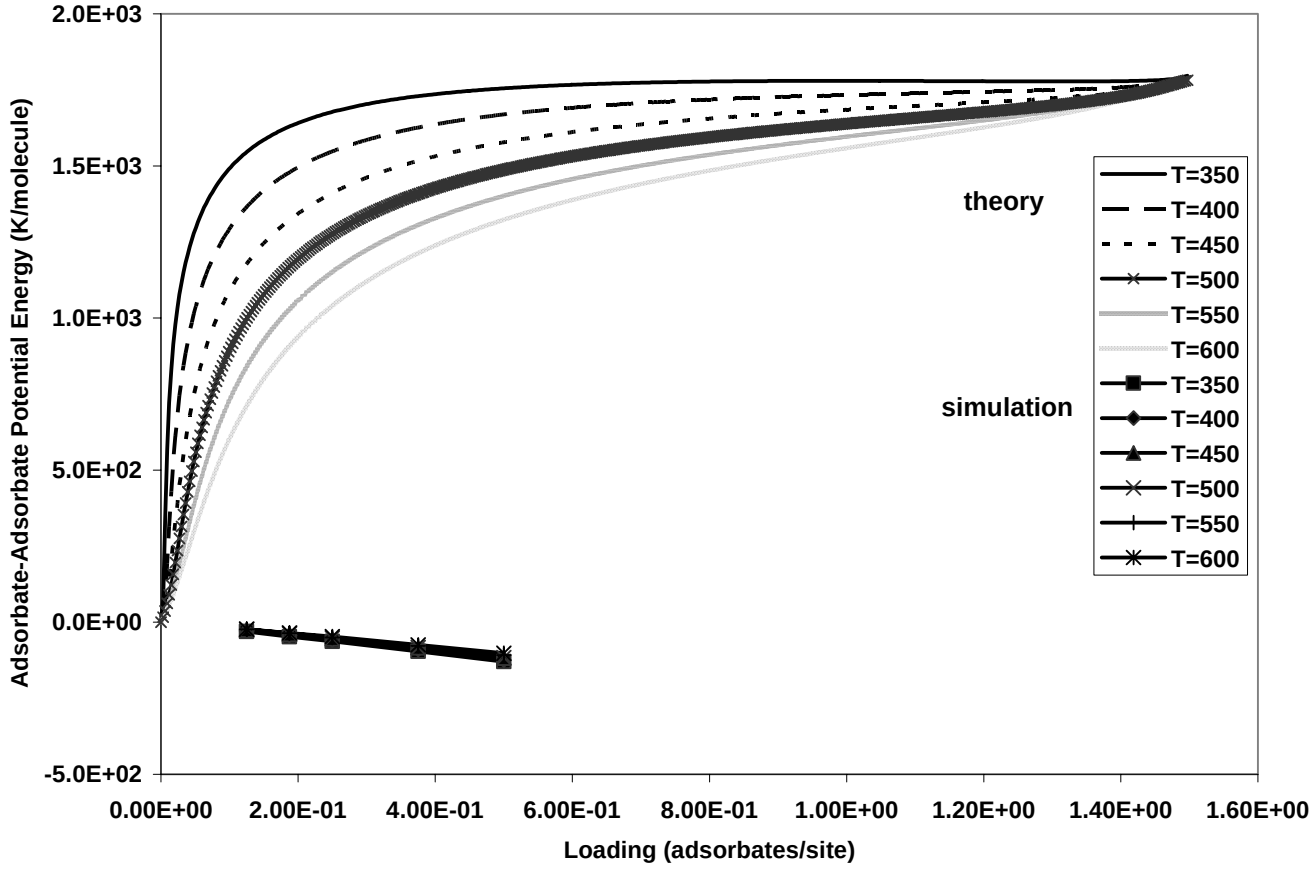

Figure (3): Adsorbate-adsorbate potential energy as a function of fractional occupancy

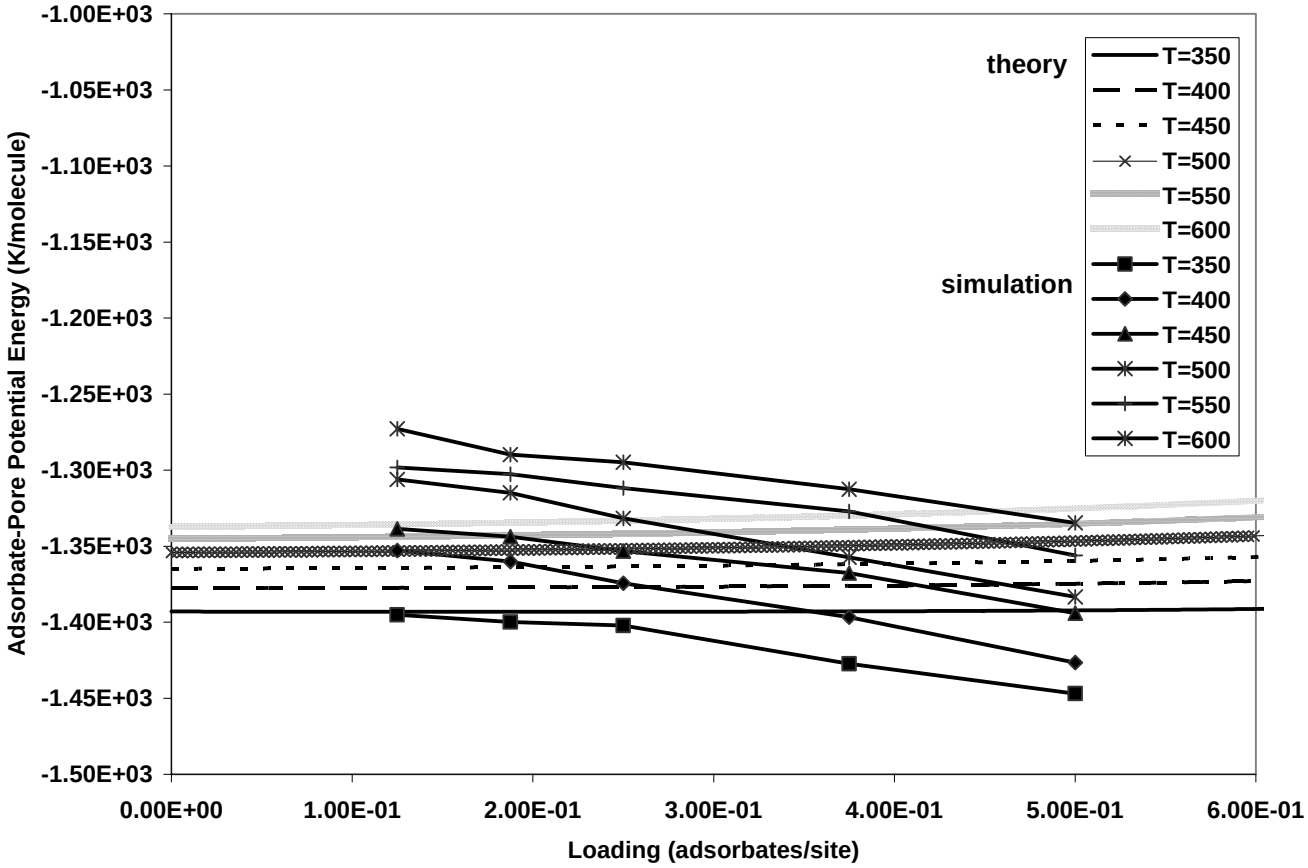

Figure (4): Adsorbate-pore interaction energy as a function of fractional occupancy

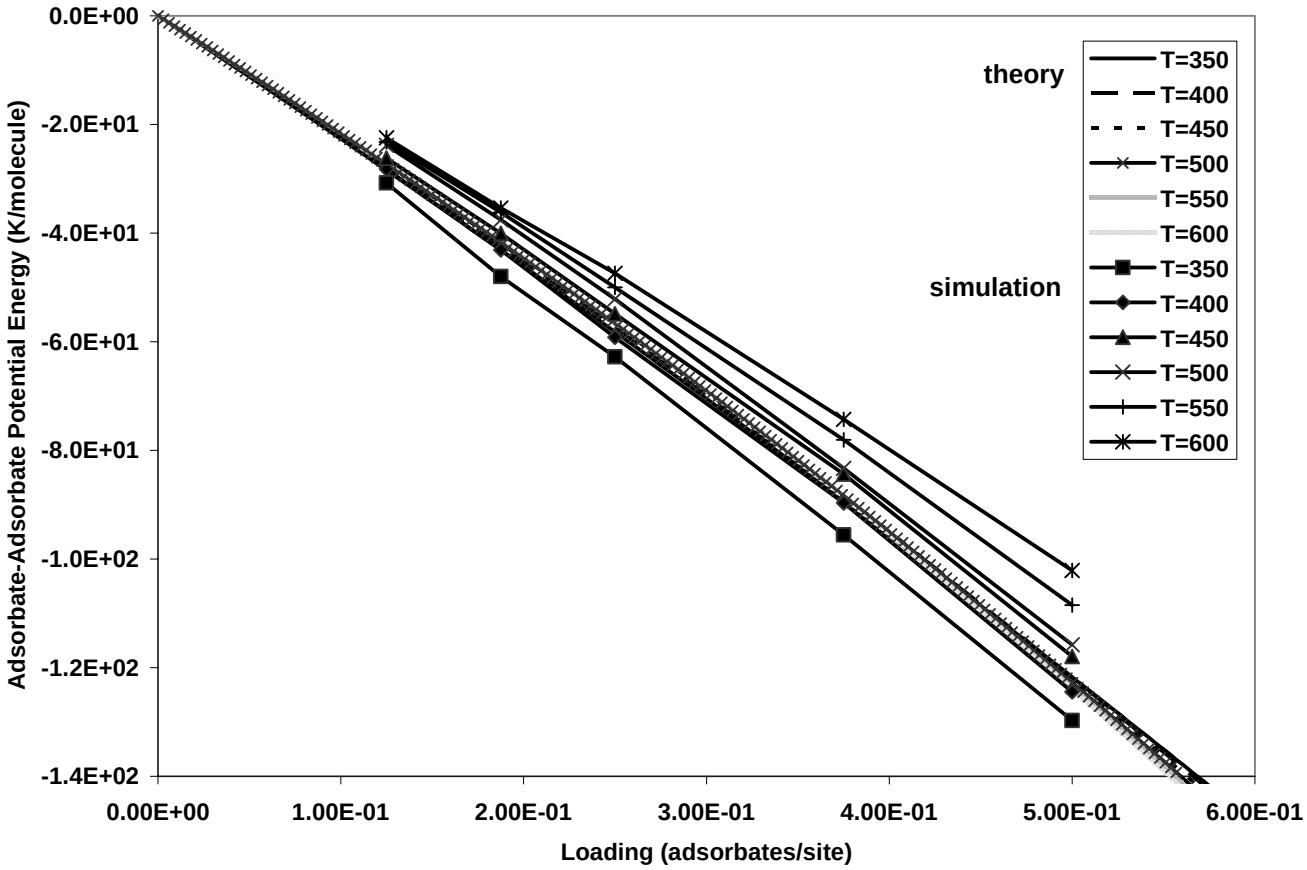

Figure (5): Adsorbate-adsorbate potential energy as a function of fractional occupancy

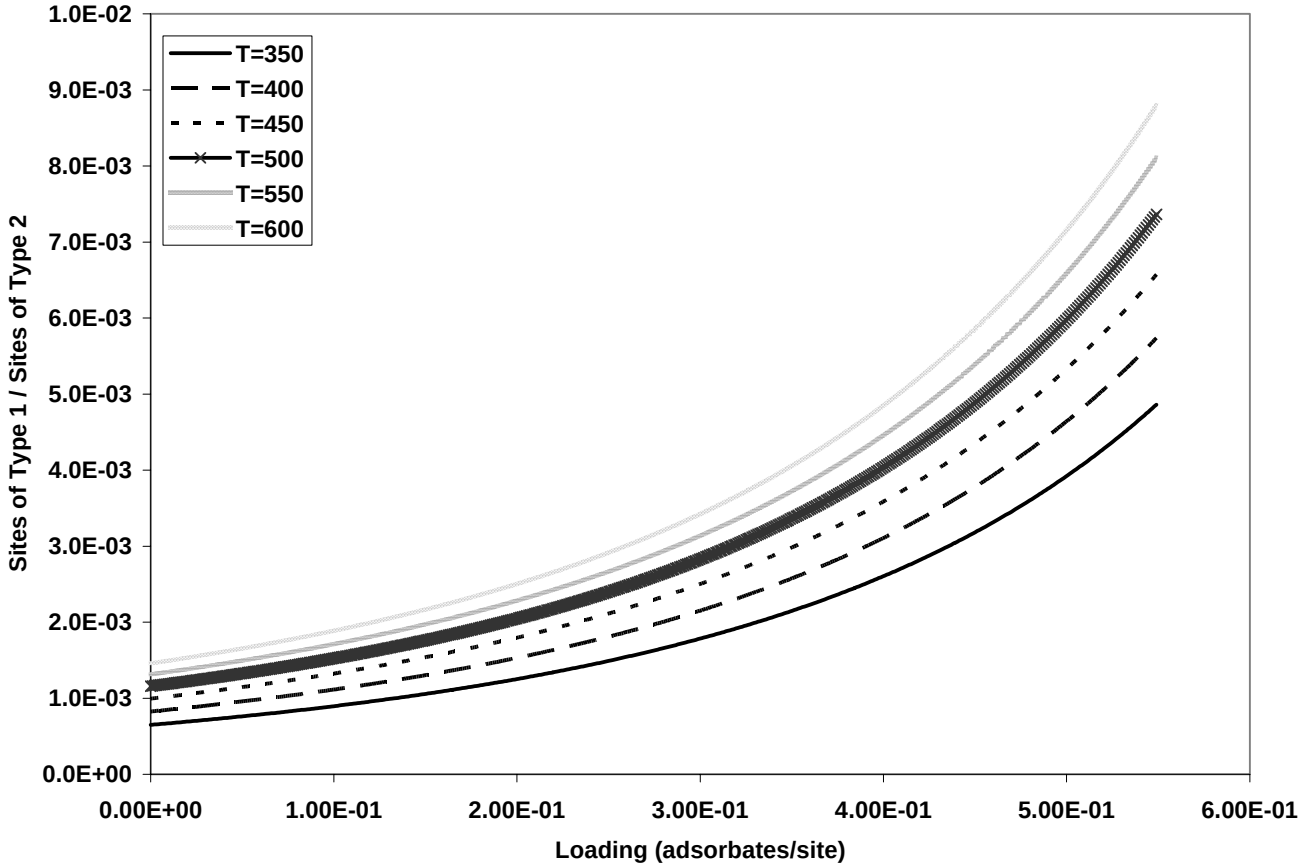

Figure (6): Ratio of sites of type 1 to sites of type 2

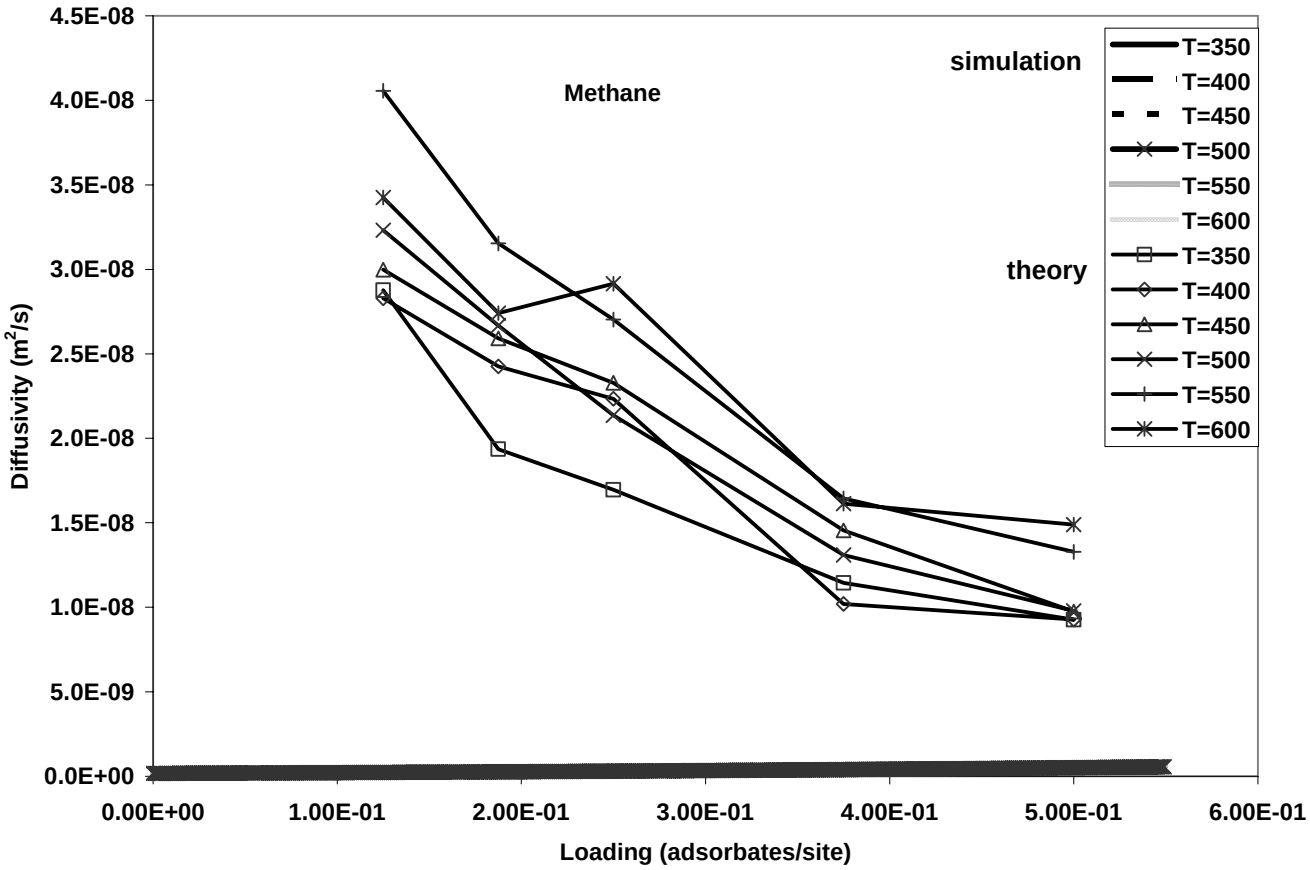

Figure (7): Methane self-diffusion coefficients as a function of fractional occupancy

Vita

Austin Newman was born on May 2nd, 1974. In 1997 Austin received his Bachelor of Science Degree with a major in Chemical Engineering from the University of Tennessee at Chattanooga. After receiving his degree, he spent several years as an engineer in the automotive industry, first with Toyoda Gosei Missouri, and then with Core Molding Technologies, Inc. In 2001 he was admitted to the University of Tennessee where he pursued the goal of obtaining the degree of Master of Science, with a major in Chemical Engineering.